Mobile-Traffic-Aware Offloading for Energy- and Spectral-Efficient Large-Scale D2D-Enabled Cellular Networks

Guogang Zhao, Sheng Chen, *Fellow, IEEE*, Lin Qi, *Member, IEEE*, Liqiang Zhao, *Member, IEEE*, and Lajos Hanzo, *Fellow, IEEE*

***Abstract*— This paper investigates how to enhance the energy and spectral efficiency (ESE) performance of large-scale cellular networks by offloading mobile traffic with the aid of device-to-device (D2D) communication. By appropriately exploiting the D2D-based mobile-traffic offloading mechanism, the users' behaviors and the specific network operating conditions, we develop an ESE evaluation framework for large-scale D2D-enabled cellular networks. This framework enables us to characterize the explicit relationship between the network's ESE and the offloading parameters as well as to quantify the influence of the users' behavior. Explicitly, we quantify the effects of the mobile-traffic intensity, the users' quality of service requirements as well as the base station density and other cellular system parameters on the achievable ESE. Tractable closed-form ESE-expressions are derived for a pair of spectrum sharing schemes, namely, D2D overlay and underlay in-band modes. Furthermore, we apply the analytical results to derive an optimal D2D-enabled mobile-traffic offloading scheme for the D2D overlay cellular networks to maximize the network's ESE under a specific maximal cellular user outage and D2D transmitter power constraint. The numerical and simulation results are provided to verify our modeling accuracy and to demonstrate the impact of the system parameters on the achievable ESE.**

Manuscript received October 18, 2017; revised August 16, 2018 and January 17, 2019; accepted April 11, 2019. Date of publication April 29, 2019; date of current version June 10, 2019. This work was supported in part by the European Research Council Advanced Fellow Grant through the Beam Me Up Project, in part by the Engineering and Physical Sciences Research Council under Grant EP/Noo4558/1 and Grant EP/L018659/1, in part by the Royal Society's Wolfson Research Merit Award, in part by the China Scholarship Council under Grant 201506960042, and in part by the State Key Program of NSFC under Grant 61331021. The work of G. Zhao was supported in part by the PhD research startup foundation of Zhengzhou University. The work of L. Zhao was supported by the National Natural Science Foundation of China (61771358), National Natural Science Foundation of Shaanxi Province (2018JM6052), and the 111 Project (B08038). The work of L. Hanzo was supported by the Engineering and Physical Sciences Research Council projects EP/Noo4558/1, EP/PO34284/1, COALESCE, of the Royal Society's Global Challenges Research Fund Grant as well as of the European Research Council's Advanced Fellow Grant QuantCom. The associate editor coordinating the review of this paper and approving it for publication was R. K. Ganti. *(Corresponding author: Lajos Hanzo.)*

G. Zhao and L. Qi are with the School of Information Engineering, Zhengzhou University, Zhengzhou 453001, China (e-mail: ggzhao@s-an.org; ielqi@zzu.edu.cn).

S. Chen is with the School of Electronics and Computer Science, University of Southampton, Southampton SO17 1BJ, U.K., and also with King Abdulaziz University, Jeddah 21589, Saudi Arabia (e-mail: sqc@ecs.soton.ac.uk).

L. Zhao is with the State Key Laboratory of Integrated Service Networks, Xidian University, Xi'an 710071, China (e-mail: lqzhao@mail.xidian.edu.cn).

L. Hanzo is with the School of Electronics and Computer Science, University of Southampton, Southampton SO17 1BJ, U.K. (e-mail: lh@ecs.soton.ac.uk).

Color versions of one or more of the figures in this paper are available online at http://ieeexplore.ieee.org.

Digital Object Identifier 10.1109/TWC.2019.2912596

***Index Terms*— Device-to-device (D2D) communication, D2D-enabled cellular network, mobile traffic offloading, spectral efficiency, energy efficiency.**

I. Introduction

DEVICE-TO-DEVICE (D2D) communication has been recognized as a significant component of supporting the emerging demands for popular local area services in the fifth-generation (5G) mobile network [1]–[3]. In a D2D-enabled cellular network, mobile devices (MDs) are allowed to directly link to other proximity devices without going through their associated base stations (BSs). Despite the increased interference caused by D2D communications, substantial performance benefits can be obtained, including more efficient resource utilization, extended cellular coverage, and enhanced network throughput. It has been widely accepted that the evolution to the 5G system should not only dramatically enhance the end-user's quality of service (QoS) and the system capacity but also significantly improve the system's energy efficiency (EE) [4]. Thus, achieving an increased performance by exploiting the energy- and spectral resources more efficiently whilst satisfying specific end-user QoS constraints is a crucial design target in the D2D-enabled cellular network.

It is worth highlighting the main reason for introducing D2D communications into the cellular network in the first place. A substantial amount of cellular spectrum and energy resources are consumed by MDs to repeatedly download an ever-increasing number of common contents from cellular BSs, such as large files containing photos or videos in social networks [5]. According to Cisco [6], the global mobile data traffic grew 63 percent in 2016, reaching 7.2 exabytes per month at the end of 2016, and it is expected to increase sevenfold between 2016 and 2021, reaching 49 exabytes per month by 2021. It is inconceivable that the existing and future cellular networks can cope with such ever-increasing amount of mobile traffic without alternative relief mechanisms. In fact, the mobile traffic offloaded to WiFi already exceeded cellular traffic in 2015 [6]. This problem can be further mitigated by offloading more of the cellular traffic to D2D communication [7]–[9].

The physical operations supporting D2D-based mobile-traffic offloading include proximity discovery, mode selection and resource allocation [10]–[14]. These operations are always coupled with the users' behaviors and with the resource/QoS-constrained physical cellular situations [5]. Therefore,

the modelling of the D2D-based mobile-traffic offloading and the evaluation of the overall energy and spectrum efficiency (ESE) performance are quite challenging [20]–[22]. Moreover, it is important to optimize the system performance by taking into account both the temporal and the geographic fluctuations of the users' behaviors as well as the time-varying physical cellular scenarios.

A. Related Works

In terms of resource utilization, such as spectrum sharing and power control, many schemes were proposed to improve the D2D communication performance [10]–[19]. For example, several resource allocation algorithms were proposed in [10] to maximize the throughput, where other system indicators, such as the maximum power constraint and rate constraints, are regarded as the constraints. The approach proposed in the study [11] maximizes the throughput while considering both the D2D and cellular link qualities as constraints. The authors of [12] developed an energy-efficient spectrum sharing strategy, which jointly considers mode selection, uplink reuse allocation and power control. We also note that the contributions [12]–[19] consider the EE or ESE as a key D2D design indicator. It can be seen that these existing works analyze the EE and spectrum efficiency aspects of D2D communication. However, their analytical results were based on the single-cell scenario with a small number of users and, therefore, can hardly be adopted in the analysis and evaluation of large-scale D2D-enabled cellular networks. Several mobile-traffic offloading methods aimed at different service types were investigated in [20]–[25], but again, these results can only be applied to a local network area.

Performance analysis and optimization of large-scale D2D-enabled cellular networks were considered in [26]–[29]. Specifically, the study [26] proposed two different power control schemes and analyzed the coverage performance in a large-scale D2D-assisted cellular network. A D2D communication framework was proposed in [27] for analyzing the signal to interference plus noise ratio distributions and the average rates. Additionally, the authors of [28] incorporated spectrum sharing and provided a comparative coverage performance analysis of two different sharing modes. Both mode selection and power control were conceived for the uplink of a large-scale D2D-enabled cellular network in [29]. However, these treatises did not analyze the influence of the temporal and geographic fluctuations of mobile traffic. By investigating a wide range of D2D communication operational conditions, including mode selection, varying maximum D2D link distances and user densities, the influence of average user rate on the achievable performance of a large-scale D2D-enabled cellular network is quantified in [30]. However, all the above-mentioned contributions focus on user-centric performance measures, such as coverage probability or achievable system capacity but they do not analyze the ESE of large-scale D2D-enabled cellular networks. Specifically, they all assume a constant power consumption in each BS and ignore the impact of mobile-traffic migration due to the offloading operation on the resource utilization and ESE. As demonstrated in our recent work [31], it is essential to adopt a realistic variable power consumption model for BSs in order to analyze and optimize the ESE of heterogeneous cellular networks.

It is quite a challenge to characterize the relationship between the mobile-traffic migration owing to D2D offloading and resource utilization whilst considering the users' large-scale behaviors. It is even more so, when facilitating offloading in large-scale D2D-enabled cellular networks and aiming for a high network-ESE performance. Hence there is a paucity of literature on this challenging subject.

B. Our Contributions

Against this backcloth, we endeavour to answer the following two fundamental questions: 1. What is the quantitative impact of the users' behavior, the physical cellular operating conditions and the offloading parameters on the network's ESE? 2. How to optimize the network's ESE by appropriately controlling the volume of geographical mobile-traffic offloaded by D2D communications, whilst satisfying the end-user's QoS requirement and power constraint?

We begin by introducing a D2D-assisted offloading mechanism for large-scale celluar networks, which takes into account both the users' behaviors and the network's operating conditions, such as the D2D offloading radius, the varying geographical mobile-traffic intensity and BS density. Our goal is to determine when and how to offload mobile traffic onto the D2D tier. Based on this offloading mechanism, we then propose an ESE evaluation framework for large-scale D2D-enabled cellular networks, which allows us to analyze the impact of the users' behaviors, the D2D-assisted offloading parameters and the cellular network operating conditions on the achievable network's ESE. Finally, we derive an optimal scenario-aware D2D-enabled offloading solution. Our main contributions are summarized below.

1) Tractable ESE Modeling for D2D-Enabled Cellular Networks: Based on the offloading mechanism conceived, we develop an ESE evaluation framework for large-scale D2D-enabled cellular networks, which allows a joint analysis of the impacts of user-behaviors, specifically, mobile-traffic intensity and average user rate, as well as of offloading strategy specified by offloading radius, of BS density and other key cellular network parameters. A pair of spectrum sharing modes, namely, the D2D overlay and underlay in-band modes (O mode and U mode), are considered.[1] Several analytical results are obtained, including the average transmit power of D2D transmitters and the network-level ESE. Finally, the qualitative impact of mobile-traffic migration between cellular communication and D2D offloading are characterized accurately. The first part of our contributions are valid for large-scale D2D-enabled cellular networks operating either in the U mode or in the O mode.

2) Energy-Spectral-Efficient D2D-Assisted Offloading Strategy for O *Mode:* For O mode, a fundamental operation issue is how the system bandwidth can be partitioned optimally into two orthogonal segments between cellular tier

[1]In U mode, both cellular tier and D2D tier share the same system bandwidth, while in O mode, they operates in the different system bandwidths orthogonally, i.e., share the system bandwidth orthogonally.

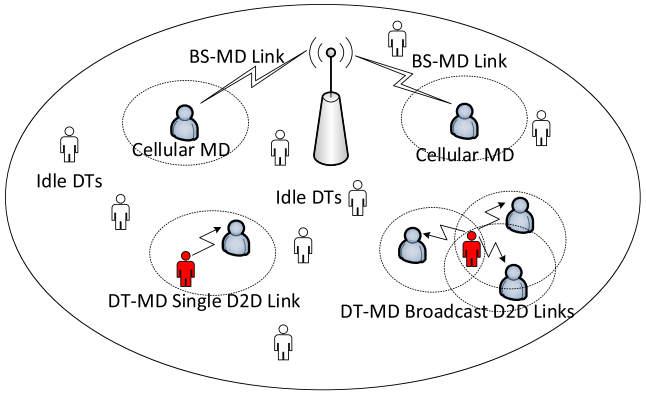

Fig. 1. Illustration of a typical cellular cell in the large-scale D2D-enabled cellular network, including two single BS-MD links, one single DT-MD link and a broadcast DT-MD link. The red DT denotes the activated DT while the white DTs are idle DTs. The dotted circles indicate the offloading decision region with each MD's location as the center.

and D2D tier. With the aid of the above-mentioned tractable analytical ESE-tool, we design an optimal D2D mobile-traffic offloading scheme for O-mode D2D enabled cellular networks to maximize the network's ESE under specific cellular user outage performance and D2D transmitter power constraints. By matching the users' behaviors and their cellular operating conditions, this optimal offloading strategy ensures the optimal spectrum sharing between the D2D tier and the cellular tier. An additional advantage of our design is its computational efficiency, since our outage-constrained and power-constrained optimal D2D-enabled offloading solution is readily given in a closed-form.

II. D2D-Enabled Cellular System Model

We consider a large-scale D2D-enabled cellular network in the downlink (DL), composed of the set of BSs $\Theta_{\rm B}$, the set of MDs $\Theta_{\rm U}$, which are retrieving their desired contents, and the set of potential D2D transmitters (DTs) $\Theta_{\rm DT}$, which are actually the MDs that currently have no content to retrieve themselves and which have been chosen by the associated BSs to relay other users' contents.[2] Any MD in $\Theta_{\rm U}$ has two service modes: cellular mode and D2D mode. Cellular MDs are associated with their geographically nearest BSs, and D2D MDs can bypass their associated BSs and directly access their DTs in their proximity. DTs are distinguished from MDs in that they either transmit radio signals to the nearby D2D MDs or stay idle. Fig. 1 depicts a typical cellular cell in such a large-scale D2D-enabled cellular network. We model $\Theta_{\rm B}$, $\Theta_{\rm U}$ and $\Theta_{\rm DT}$ with three independent Poisson point processes (PPPs) in the Euclidean plane $\mathbb{R}^2$ with the intensities $\lambda_{\rm B}$, $\lambda_{\rm U}$ and $\lambda_{\rm DT}$, respectively. We consider both the large-scale pathloss and small-scale fast fading for each desired or interference signal. More specifically, the large-scale pathloss is modeled by $l = d^{-\alpha}$ with d denoting the distance between the transmitter and receiver and α being the pathloss exponent. Rayleigh-distributed fast-fading is considered. In our analysis, the effect of the noise is ignored, since the interference power is far higher than the noise power in this interference-limited scenario.[3]

Each MD $u_i \in \Theta_{\rm U}$ has to make an offloading decision, either retrieving its content in its cellular mode or via its D2D mode. This decision depends on the distribution state of the DTs in its proximity. Let the effective D2D transmission range or radius be $\varpi_{\rm D}$, which is defined by

$$\varpi_{\rm D}^{-\alpha} = \nu[\%], \tag{1}$$

i.e., it is defined as the distance at which the pathloss causes the signal power to drop to $\nu\%$. Then, u_i has an offloading region $\mathbb{O}\big(u_i, \varpi_{\rm D}\big)$, which is the disc with u_i as the center and the radius $\varpi_{\rm D}$. Let $N_{\mathbb{O}_{u_i}}$ denote the number of DTs located inside $\mathbb{O}\big(u_i, \varpi_{\rm D}\big)$. Since the objective is to maximally offload mobile traffic to the D2D tier while maintaining certain user QoS requirements, u_i is in its D2D mode, whenever $N_{\mathbb{O}_{u_i}} \geq 1$, and it has to opt for its cellular mode if $N_{\mathbb{O}_{u_i}} = 0$. Furthermore, a MD u_i with D2D mode always choose the nearest DT inside $\mathbb{O}\big(u_i, \varpi_{\rm D}\big)$ to retrieve its content. Thus, we can define the mobile-traffic offloading probability as $P_{\rm OL} = \Pr\left(N_{\mathbb{O}_{u_i}} \geq 1\right)$, which effectively divides all the MDs into the subset of cellular MDs $\Theta_{\rm U}^C$ and the subset of D2D MDs $\Theta_{\rm U}^D$. We further assume that each DT can serve multiple MDs by broadcasting the offloaded traffic, and the activation of other idle DT will not prevent it from receiving the offloading requests from its proximate potential MDs. This assumption implies that there is no correlation in establishing different DT-MD links. Consequently, $\Theta_{\rm U}^C$ and $\Theta_{\rm U}^D$ follow the two independent thinned PPPs with the densities of $(1 - P_{\rm OL})\lambda_{\rm U}$ and $P_{\rm OL}\lambda_{\rm U}$, respectively.

For a typical BS $b_j \in \Theta_{\rm B}$, we define its service or coverage area by $S_{A,j}$. The maximum number of cellular MDs supported in each cell is N_C. Furthermore, we denote the set of all the MDs under the coverage area $S_{A,j}$ by $\Theta_{\rm U}^j$. Clearly, $\Theta_{\rm U}^j \cap \Theta_{\rm U}^{j'} = \emptyset$ for $j \neq j'$ and $\cup_{b_j \in \Theta_{\rm B}} \Theta_{\rm U}^j = \Theta_{\rm U}$. The MDs of $\Theta_{\rm U}^j$ can be divided into two groups, cellular MDs, collected in the subset $\Theta_{\rm U}^{C,j} = \left\{u_i^{C,j}\right\}_{i=1}^{N_C}$, and D2D MDs, collected in the subset $\Theta_{\rm U}^{D,j}$. Obviously, $\Theta_{\rm U}^{C,j} \cup \Theta_{\rm U}^{D,j} = \Theta_{\rm U}^j$. The system bandwidth of W [Hz] is reused spatially in every cell.

For the U mode, both the cellular and D2D tiers share the same system bandwidth of W [Hz] in each cell. The total bandwidth of W [Hz] is divided into the N_C subbands to be allocated to the MDs in $\Theta_{\rm U}^{C,j}$. The same system bandwidth of W [Hz] is divided into $\beta \in \mathbb{N}^+$ subbands in the D2D tier for the D2D pairs to access.[4] Each D2D pair in $\Theta_{\rm U}^{D,j}$, which is associated with BS b_j, can randomly and independently

[2]In this work, we assume that the set of DTs $\Theta_{\rm DT}$ has been selected. How to select DTs or D2D relays is a very complicated problem. This is because many factors, including instantaneous link conditions, spectrum sharing mode, resource allocation and interference mitigation technique adopted, must be taken into consideration. Moreover, mobility patterns and social network features can be utilized to select better D2D relays [5], [22], [32]–[34].

[3]It is well known that in this circumstance, the noise power only has a very marginal effect on the system coverage probability [35] and almost has no influence on the network EE [36].

[4]Each D2D MD $u_i^{D,j} \in \Theta_U^{D,j}$ is obviously associated with a DT or DT-MD link. For convenience, we refer to $u_i^{D,j}$ and its associated DT as a D2D pair in $\Theta_U^{D,j}$.

access one subband to reduce the interference imposed on the other links in the same cell. Note that the probability to access a subband by a D2D pair is $1/\beta$. Therefore, $1/\beta$ can be considered as the access probability of D2D pairs, which measures the intensity of D2D bandwidth access. Since D2D link should supports higher-rate than cellular link, the subband allocated to a cellular MD is narrower than that accessed by a D2D MD, and we have $N_C > \beta$.

For the O mode, the total bandwidth is divided into two orthogonal segments. The fraction of $(1-\omega)W$ is allocated to the cellular tier, and the other part of ωW is used for the D2D tier, where $0 < \omega < 1$. Specifically, the cellular-tier bandwidth $(1-\omega)W$ is divided into the N_C subbands for the MDs of $\Theta_{\mathrm{U}}^{C,j}$, while the D2D-tier bandwidth ωW is divided into the β subbands for the D2D pairs of $\Theta_{\mathrm{U}}^{D,j}$. Similarly, the subband allocated to a cellular MD is typically narrower than that for a D2D MD.

First, let us consider a typical BS-MD link between b_j and the i-th cellular MD $u_i^{C,j} \in \Theta_{\mathrm{U}}^{C,j}$, where $1 \le i \le N_C$. The link service rate satisfies

$$R_i^{C,j} = W_C \log_2\left(1 + \frac{P_i^{C,j} l_i^{C,j} h_i^{C,j}}{I_j^{CC} + I_j^{DC}}\right), \tag{2}$$

where $W_C = W/N_C$ for the U mode and $W_C = (1-\omega)W/N_C$ for the O mode, $P_i^{C,j} \le P_C/N_C$ is the required transmit power allocated to the subband of this cellular link with P_C denoting the maximum transmission power of the BS, while $l_i^{C,j} = \left\|u_i^{C,j} - b_j\right\|^{-\alpha}$ is the pathloss and $h_i^{C,j}$ denotes the fast-fading power gain of the channel between b_j and $u_i^{C,j}$, which is exponentially distributed with a unity mean, i.e., $h_i^{C,j} \sim \exp(1)$. Furthermore, we consider the worst-case interference, where all interfering BSs transmit at the maximum power P_C/N_C at the subband. Hence, for both the U mode and O mode, the interference coming from all the other BSs' transmissions is given by

$$I_j^{CC} = \sum_{b_m \in \{\Theta_{\mathrm{B}} \setminus b_j\}} \frac{P_C}{N_C} h_i^{C,m} l_i^{C,m}. \tag{3}$$

Similarly, let us assume that all the interfering DTs transmit at the maximum power of P_D/β at a subband, where P_D is the maximum transmission power of DT. Then for the U mode, the worst-case interference coming from all the interfering DTs can be expressed as

$$I_j^{DC} = \sum_{\mathrm{DT}_n \in \overline{\mathbb{O}}\left(u_i^{C,j}, \varpi_{\mathrm{D}}\right), \left(\mathrm{DT}_n \wedge u_i^{C,j}\right)} \frac{P_D}{N_C} h_i^{D,n} l_i^{D,n}, \tag{4}$$

where P_D/N_C is the power of the interfering D2D transmissions inside the celluar subband for $u_i^{C,j}$, $l_i^{D,n} = \left\|u_i^{C,j} - \mathrm{DT}_n\right\|^{-\alpha}$ and $h_i^{D,n}$ are respectively the pathloss and fast fading power gain of the link between DT_n and $u_i^{C,j}$, while $\overline{\mathbb{O}}\left(u_i^{C,j}, \varpi_{\mathrm{D}}\right)$ denotes the exclusive region to the offloading region $\mathbb{O}\left(u_i^{C,j}, \varpi_{\mathrm{D}}\right)$ and $\left(\mathrm{DT}_n \wedge u_i^{C,j}\right)$ indicates that the D2D subband for DT_n overlaps with the cellular subband for $u_i^{C,j}$. Note that in the cellular mode, there exists no DT in $\mathbb{O}\left(u_i^{C,j}, \varpi_{\mathrm{D}}\right)$. For the O mode, obviously,

$$I_j^{DC} = 0. \tag{5}$$

Because the worst-case interference is considered, the service rate of (2) represents a low bound of the achievable rate.

Second, for the k-th D2D MD $u_k^{D,j}$ located inside $S_{A,j}$, let $\mathrm{DT}_n \in \mathbb{O}\left(u_k^{D,j}, \varpi_{\mathrm{D}}\right)$ be the nearest DT. Then the service rate of the link between DT_n and $u_k^{D,j}$ satisfies

$$R_k^{D,n} = W_D \log_2\left(1 + \frac{P_k^{D,n} l_k^{D,n} h_k^{D,n}}{I_n^{CD} + I_n^{DD}}\right), \tag{6}$$

where $W_D = W/\beta$ for the U mode and $W_D = \omega W/\beta$ for the O mode, while $P_k^{D,n} \le P_D/\beta$ is the required transmit power allocated to the subband of this D2D link. In (6), $l_k^{D,n}$ and $h_k^{D,n}$ are the pathloss and fast fading power gain of the link between DT_n and $u_k^{D,j}$, respectively. For the U mode, the worst-case interference coming from all the celluar transmissions is given by

$$I_n^{CD} = \sum_{b_m \in \Theta_{\mathrm{B}}} \frac{P_C}{\beta} h_k^{C,m} l_k^{C,m}, \tag{7}$$

where P_C/β is the power of the interfering celluar transmissions inside the D2D subband for $u_k^{D,j}$, while $l_k^{C,m}$ and $h_k^{C,m}$ are the pathloss and fast fading power gain of the link between b_m and $u_k^{D,j}$, respectively. For the O mode, clearly,

$$I_n^{CD} = 0. \tag{8}$$

Furthermore, denote $l_k^{D,n'}$ and $h_k^{D,n'}$ as the pathloss and fast fading power gain of the link between $\mathrm{DT}_{n'}$ and $u_k^{D,j}$, respectively. Then, for both the U mode and O mode, the worst-case interference coming from all the other D2D transmissions can be expressed as

$$I_n^{DD} = \sum_{n' \ne n, \left(\mathrm{DT}_{n'} \overline{\wedge} \mathrm{DT}_n\right)} \frac{P_D}{\beta} h_k^{D,n'} l_k^{D,n'}, \tag{9}$$

where $\left(\mathrm{DT}_{n'} \overline{\wedge} \mathrm{DT}_n\right)$ indicates that $\mathrm{DT}_{n'}$ and DT_n are allocated with the same D2D subband. Again, the service rate of (6) represents a low bound of the achievable rate.

Table I lists the main notations used in this paper.

III. ESE Evaluation of Large-Scale Mobile-Traffic-Aware D2D-Enabled Offloading

In this section, we first model the large-scale mobile-traffic-aware D2D-assisted offloading by appropriately configuring the offloading region at each MD in both the U and O modes, and then quantify the overall ESE performance based on the network's resource utilization in both the D2D and cellular tiers for a large-scale D2D-enabled cellular network.

A. Offloading Region for D2D-Enabled Offloading

Modeling offloading region is the first step in the ESE performance evaluation of a large-scale D2D-enabled offloading system. Therefore, we firstly characterize the effective D2D transmission radius by considering the requirement for the transmit power capability of D2D transmitter, measured in watt. Hence, the following two propositions are given.

TABLE I
LIST OF MAIN NOTATIONS

Notation	Definition
$\Theta_{\rm B}$, $\Theta_{\rm U}$, $\Theta_{\rm DT}$	Sets of BSs, MDs, DTs
$\lambda_{\rm B}$, $\lambda_{\rm U}$, $\lambda_{\rm DT}$	BS density, MD density, DT density
$\varpi_{\rm D}$	Offloading radius
$P_{\rm OL}$	Offloading probability
$S_{A,j}$	Coverage area of typical BS b_j
$\Theta_{\rm U}^{j}$	Set of MDs covered by b_j
$\Theta_{\rm U}^{C,j}$, $\Theta_{\rm U}^{D,j}$	Sets of cellular MDs, D2D MDs covered by b_j
N_C	Maximum number of cellular MDs served by b_j
W	Total system bandwidth in Hz
α	Pathloss exponent
$1/\beta$	D2D access probability
ω	Faction of system bandwidth for O mode D2D tier
$R_i^{C,j}$	Service rate of typical BS-MD link
$R_k^{D,n}$	Service rate of typical DT-MD link
$R_{\rm C}$	Average service rate of typical BS-MD link
$R_{\rm D2D}$	Average service rate of typical DT-MD link
P_C, P_D	Maximum transmit powers of BSs and DTs
$l_i^{C,j}$, $h_i^{C,j}$	Pathloss and fading gain between b_j and $u_i^{C,j}$
$l_k^{D,n}$, $h_k^{C,n}$	Pathloss and fading gain between DT$_n$ and $u_k^{D,j}$
$P_i^{C,j}$	Transmit power for the link between b_j and $u_i^{C,j}$
$P_k^{D,n}$	Transmit power for the link between DT$_n$ and $u_k^{D,j}$
$\eta_{\rm ESE}^{\rm O}$, $\eta_{\rm ESE}^{\rm U}$	Network ESEs in O and U modes
$a_{\rm E}$, $b_{\rm E}$	Efficiency factors of power amplifiers at BS and DT
$\mathcal{K}$	DT active probability
$P_{\rm D_a}^{\rm O}$, $P_{\rm D_a}^{\rm U}$	Average D2D transmit powers in O and U modes
$P_{\rm CJ}^{\rm O}$, $P_{\rm CJ}^{\rm U}$	Average transmit powers of b_j to $u_i^{C,j}$ in two modes
$P_{\rm BS}^{\rm O}$, $P_{\rm BS}^{\rm U}$	Aggregate transmit powers of BS b_j in two modes

Proposition 1: In a large-scale D2D-enabled U-mode based cellular network having a BS density of $\lambda_{\rm B}$, a mobile-traffic intensity of $\lambda_{\rm U}$ and a DT density of $\lambda_{\rm DT}$, the transmit power capability of D2D transmitters, denoted by $\mathrm{Z}_{\rm U}^{\rm D}$ [watt], the average D2D user rate $R_{\rm D2D}$, the D2D access probability $1/\beta$, and the effective D2D transmission radius $\varpi_{\rm D}$, which defines the offloading region $\mathbb{O}\big(u_i, \varpi_{\rm D}\big)$ in the U mode, satisfy the following inequality, (10), shown at the bottom of this page, where $\alpha > 2$, $P_{\rm OL}$ is the offloading probability given by

$$P_{\rm OL} = \Pr\left(N_{\mathbb{O}_{u_i}} \geq 1\right) = 1 - \exp\left(-\pi\lambda_{\rm DT}\varpi_{\rm D}^2\right), \quad (11)$$

$\gamma(a,x)$ is the incomplete Gamma function expressed as

$$\gamma(a,x) = \int_0^x t^{a-1}\exp(-t)\,dt, \quad (12)$$

and $\Gamma(x) = \int_0^{+\infty} t^{x-1}\exp(-t)dt$, while the DT active probability $\mathcal{K}$, a function of $\lambda_{\rm U}$ and $\varpi_{\rm D}$, is given by

$$\mathcal{K} = \big(\mathrm{Ei}(y) - \mathrm{Ei}(1) - \ln y + 1.3179\big)\exp(-y) \leq 1, \quad (13)$$

with $y = \pi\lambda_{\rm U}\varpi_{\rm D}^2$ and $\mathrm{Ei}(y)$ being the exponential integral function defined by

$$\mathrm{Ei}(y) = -\int_{-y}^{\infty} \frac{\exp(-t)}{t}\,dt. \quad (14)$$

Clearly, the maximum tolerable D2D transmission radius $\varpi_{\rm D\,max}^{\rm U}$ corresponding to $\mathrm{Z}_{\rm U}^{\rm D}$ can be numerically obtained by setting $\varpi_{\rm D} = \varpi_{\rm D\,max}^{\rm U}$ and replacing '$\geq$' with '$=$' in (10).

Proof: See Appendix A. ■

Remark 1: The right-hand side of the inequality (10) defines the D2D transmit power requirement in the U mode.

1) Since increasing β leads to exponential increase of $P_{\rm D_a}^{\rm U}$, the D2D transmit power capability is a monotonically increasing function of β. Thus, using narrower subbands in the D2D tier reduces $P_{\rm D_a}^{\rm U}$ and hence $\mathrm{Z}_{\rm U}^{\rm D}$.
2) From (10), $P_{\rm D_a}^{\rm U}$ is a monotonically increasing function of $\lambda_{\rm DT}$. This is because increasing the DT density $\lambda_{\rm DT}$ directly increases the interference because of more active D2D pairs.
3) According to (10), to increase the effective D2D radius $\varpi_{\rm D}$ requires a corresponding increase in the D2D transmit power capability $\mathrm{Z}_{\rm U}^{\rm D}$, which also makes sense.

Proposition 2: In a large-scale D2D-enabled O-mode based cellular network having the total bandwidth ωW in the D2D tier, a mobile-traffic intensity of $\lambda_{\rm U}$ and a DT density of $\lambda_{\rm DT}$, the D2D transmit power capability $\mathrm{Z}_{\rm O}^{\rm D}$ [watt], the average user rate $R_{\rm D2D}$, the D2D access probability $1/\beta$, and the effective D2D transmission radius $\varpi_{\rm D}$, which characterizes the offloading region $\mathbb{O}\big(u_i, \varpi_{\rm D}\big)$ in the O mode, satisfy the following inequality

$$\mathrm{Z}_{\rm O}^{\rm D} \geq P_{\rm D_a}^{\rm O} \triangleq \left(2^{\frac{\beta R_{\rm D2D}}{\omega W}} - 1\right)\frac{2\pi\mathcal{K}P_D\lambda_{\rm U}P_{\rm OL}}{\beta(\alpha-2)} \times \left(\frac{P_{\rm OL}}{\pi\lambda_{\rm DT}} - \frac{\varpi_{\rm D}^2}{\exp\left(\pi\lambda_{\rm DT}\varpi_{\rm D}^2\right)}\right), \quad (15)$$

where $\alpha > 2$. Furthermore, the maximum tolerable D2D transmission radius $\varpi_{\rm D\,max}^{\rm O}$ related to $\mathrm{Z}_{\rm O}^{\rm D}$ can be numerically obtained by setting $\varpi_{\rm D} = \varpi_{\rm D\,max}^{\rm O}$ and replacing '$\geq$' with '$=$' in (15).

Proof: See Appendix B. ■

Remark 2: Different from the U mode, the D2D transmit power capability $\mathrm{Z}_{\rm O}^{\rm D}$ in the O mode is independent of $\lambda_{\rm B}$, since the cross-tier interference is eliminated in an orthogonal spectrum sharing. Similar to the case of U mode, to increase the effective D2D transmission radius $\varpi_{\rm D}$ in the O mode requires a corresponding increase in the D2D transmit power capability $\mathrm{Z}_{\rm O}^{\rm D}$.

B. Downlink Transmit Power Analysis

Next we derive the average DL transmit power for a typical BS-MD link and the BS's aggregate DL transmit power in both the U and O modes.

Proposition 3: In a large-scale D2D-enabled cellular network having a BS density of $\lambda_{\rm B}$ with the average cellular user rate $R_{\rm C}$, a mobile-traffic intensity of $\lambda_{\rm U}$ and a DT density of $\lambda_{\rm DT}$ with the D2D offloading radius $\varpi_{\rm D}$, the average DL

$$\mathrm{Z}_{\rm U}^{\rm D} \geq P_{\rm D_a}^{\rm U} \triangleq \left(2^{\frac{\beta R_{\rm D2D}}{W}} - 1\right)\left(\frac{2\pi\mathcal{K}P_D\lambda_{\rm U}P_{\rm OL}}{(\alpha-2)\beta}\left(\frac{P_{\rm OL}}{\pi\lambda_{\rm DT}} - \frac{\varpi_{\rm D}^2}{\exp\left(\pi\lambda_{\rm DT}\varpi_{\rm D}^2\right)}\right) + \frac{2\lambda_{\rm B}^{\frac{\alpha}{2}}P_C}{(\alpha-2)\beta\lambda_{\rm DT}^{\frac{\alpha}{2}}}\Gamma\left(2-\frac{\alpha}{2}\right)\gamma\left(\frac{\alpha+2}{2}, \pi\lambda_{\rm DT}\varpi_{\rm D}^2\right)\right), \quad (10)$$

transmit power assigned in W_C for a typical BS-MD link in the U mode is given by

$$P_{\mathrm{C1}}^{\mathrm{U}} = \frac{\left(2^{\frac{R_{\mathrm{C}}}{W_C}}-1\right)2\lambda_{\mathrm{B}}}{(\alpha-2)\exp\left(-\pi\lambda_{\mathrm{DT}}\varpi_{\mathrm{D}}^2\right)\lambda_{\mathrm{U}}} \times \left(P_C + \frac{\alpha\Gamma\left(\frac{\alpha}{2}\right)\pi^{\frac{2-\alpha}{2}}P_D\lambda_{\mathrm{U}}\mathcal{K}P_{\mathrm{OL}}}{2\lambda_{\mathrm{B}}^{\frac{\alpha}{2}}\varpi_{\mathrm{D}}^{\alpha-2}}\right), \quad (16)$$

where $\alpha > 2$. Furthermore, assuming that all the cellular MDs have an identical user rate of R_{C}, the BS's aggregate DL transmit power in the U mode is given as

$$P_{\mathrm{BS}}^{\mathrm{U}} = \frac{\left(2P_C\lambda_{\mathrm{B}}^{\frac{\alpha}{2}}\varpi_{\mathrm{D}}^{\alpha-2} + \alpha\Gamma\left(\frac{\alpha}{2}\right)\pi^{\frac{2-\alpha}{2}}P_D\lambda_{\mathrm{U}}\mathcal{K}P_{\mathrm{OL}}\right)K^K}{(\alpha-2)\left(K-\left(2^{\frac{R_{\mathrm{C}}}{W_C}}-1\right)(1-P_{\mathrm{OL}})\frac{\lambda_{\mathrm{U}}}{\lambda_{\mathrm{B}}}\right)^K\lambda_{\mathrm{B}}^{\frac{\alpha}{2}}\varpi_{\mathrm{D}}^{\alpha-2}} - \frac{2P_C}{(\alpha-2)} - \frac{\alpha\Gamma\left(\frac{\alpha}{2}\right)\pi^{\frac{2-\alpha}{2}}P_D\lambda_{\mathrm{U}}\mathcal{K}P_{\mathrm{OL}}}{(\alpha-2)\lambda_{\mathrm{B}}^{\frac{\alpha}{2}}\varpi_{\mathrm{D}}^{\alpha-2}}, \quad (17)$$

where $K = 3.75$.

Proof: See Appendix C. ∎

Remark 3: The influence of λ_{DT} to $P_{\mathrm{C1}}^{\mathrm{U}}$ is complicated. Increasing λ_{DT} decreases $\exp\left(-\pi\lambda_{\mathrm{DT}}\varpi_{\mathrm{D}}^2\right)$ but increases P_{OL}. From (16), it is seen that $P_{\mathrm{C1}}^{\mathrm{U}}$ contains both $\exp\left(-\pi\lambda_{\mathrm{DT}}\varpi_{\mathrm{D}}^2\right)$ and P_{OL}. However, increasing λ_{DT} also decreases W_C, since the average of W_C is $E[W_C] \approx W\lambda_{\mathrm{B}}(1-P_{\mathrm{OL}})/\lambda_{\mathrm{U}} = W\lambda_{\mathrm{B}}\exp\left(-\pi\lambda_{\mathrm{DT}}\varpi_{\mathrm{D}}^2\right)/\lambda_{\mathrm{U}}$, which increases $P_{\mathrm{C1}}^{\mathrm{U}}$. Therefore, the overall effect of increasing λ_{DT} is to increase $P_{\mathrm{C1}}^{\mathrm{U}}$. The influence of ϖ_{D} to $P_{\mathrm{C1}}^{\mathrm{U}}$ is also complicated. Increasing ϖ_{D} decreases $\exp\left(-\pi\lambda_{\mathrm{DT}}\varpi_{\mathrm{D}}^2\right)$ but increases P_{OL}. However, $P_{\mathrm{C1}}^{\mathrm{U}}$ contains $\varpi_{\mathrm{D}}^{2-\alpha}$ with $\alpha > 2$, which decreases as ϖ_{D} increases. Hence, overall, increasing ϖ_{D} reduces $P_{\mathrm{C1}}^{\mathrm{U}}$. Moreover, $P_{\mathrm{C1}}^{\mathrm{U}}$ contains the factor of $\frac{1}{\lambda_{\mathrm{U}}}$, but increasing $\frac{1}{\lambda_{\mathrm{U}}}$ can increase W_C which will reduce $P_{\mathrm{C1}}^{\mathrm{U}}$. Therefore, the overall effect of increasing $\frac{1}{\lambda_{\mathrm{U}}}$ is to decrease $P_{\mathrm{C1}}^{\mathrm{U}}$.

Proposition 4: In a large-scale D2D-enabled cellular network having a BS density of λ_{B} with the average cellular user rate R_{C}, a mobile-traffic intensity of λ_{U} and a DT density λ_{DT} with the D2D offloading radius ϖ_{D}, given the total bandwidth in cellular tier $(1-\omega)W$, the average DL transmit power assigned in W_{C} for a typical BS-MD link in the O mode is given by

$$P_{\mathrm{C1}}^{\mathrm{O}} = \frac{2P_{\mathrm{C}}\lambda_{\mathrm{B}}\left(2^{\frac{R_{\mathrm{C}}}{W_C}}-1\right)}{(\alpha-2)\exp\left(-\pi\lambda_{\mathrm{DT}}\varpi_{\mathrm{D}}^2\right)\lambda_{\mathrm{U}}}. \quad (18)$$

Furthermore, assuming that all the cellular MDs have an identical service rate of R_{C}, the BS's aggregate DL transmit power in the O mode is given by

$$P_{\mathrm{BS}}^{\mathrm{O}} = \frac{2P_{\mathrm{C}}K^K\lambda_{\mathrm{B}}^K\left(\exp\left(\pi\lambda_{\mathrm{DT}}\varpi_{\mathrm{D}}^2\right)\right)^K}{(\alpha-2)\left(K\lambda_{\mathrm{B}}\exp\left(\pi\lambda_{\mathrm{DT}}\varpi_{\mathrm{D}}^2\right)-\left(2^{\frac{R_{\mathrm{C}}}{(1-\omega)W}}-1\right)\lambda_{\mathrm{U}}\right)^K} - \frac{2P_{\mathrm{C}}}{(\alpha-2)}. \quad (19)$$

Proof: The proof is similar to the proof of Proposition 3. In fact, the proof is simpler, as the cross-tier interference $I_j^{DC} = 0$ in the O mode. ∎

C. Network ESE Performance Evaluation

We now quantify the network's ESE. First, the network's area power consumptions (APCs) from all the BS-MD links in the U and O modes are given respectively by

$$\mathcal{C}_{\mathrm{BS}}^{\mathrm{U}} = a_{\mathrm{E}}P_{\mathrm{BS}}^{\mathrm{U}}\lambda_{\mathrm{B}} + P_{\mathrm{OM}}\lambda_{\mathrm{B}}\ [\mathrm{watt/m^2}], \quad (20)$$

$$\mathcal{C}_{\mathrm{BS}}^{\mathrm{O}} = a_{\mathrm{E}}P_{\mathrm{BS}}^{\mathrm{O}}\lambda_{\mathrm{B}} + P_{\mathrm{OM}}\lambda_{\mathrm{B}}\ [\mathrm{watt/m^2}], \quad (21)$$

where a_{E} is the efficiency factor of BS power amplifier and P_{OM} is the static operation power consumption of a BS. Second, the APCs from all the D2D links in the U and O modes are given respectively by

$$\mathcal{C}_{\mathrm{D2D}}^{\mathrm{U}} = b_{\mathrm{E}}\lambda_{\mathrm{DT}}^{\mathrm{act}}P_{\mathrm{D_a}}^{\mathrm{U}}\ [\mathrm{watt/m^2}], \quad (22)$$

$$\mathcal{C}_{\mathrm{D2D}}^{\mathrm{O}} = b_{\mathrm{E}}\lambda_{\mathrm{DT}}^{\mathrm{act}}P_{\mathrm{D_a}}^{\mathrm{O}}\ [\mathrm{watt/m^2}], \quad (23)$$

where b_{E} is the efficiency factor of DT power amplifier, and $\lambda_{\mathrm{DT}}^{\mathrm{act}} = \mathcal{K}\lambda_{\mathrm{U}}P_{\mathrm{OL}}$ is the active DT density (see Appendix A). Note that in (20) to (23), the receiver signal processing power consumption is neglected.[5] By using R_{C} and R_{D2D} to denote the average user rates in cellular and D2D tiers, respectively, the network's area spectral efficiency (ASE) is given by

$$\mathcal{S} = \frac{\lambda_{\mathrm{U}}}{W}\left((1-P_{\mathrm{OL}})R_{\mathrm{C}} + P_{\mathrm{OL}}R_{\mathrm{D2D}}\right)\ [\mathrm{bit/s/Hz/m^2}]. \quad (24)$$

We are ready to present the ESE performance of the large-scale D2D-enabled cellular network operating in the U and O modes in the following two propositions, respectively.

Proposition 5: For the large-scale D2D-enabled cellular network operating in the U mode with the cellular and D2D spatially average user rates of R_{C} and R_{D2D}, respectively, as well as having a BS density of λ_{B}, a mobile-traffic intensity of λ_{U}, a DT density λ_{DT} with the D2D offloading radius ϖ_{D}, the BS static operation power consumption P_{OM}, and the BS and DT power amplifier efficiencies of a_{E} and b_{E}, respectively, the network's ESE is expressed as

$$\eta_{\mathrm{ESE}}^{\mathrm{U}} = \frac{\mathcal{S}}{\mathcal{C}_{\mathrm{BS}}^{\mathrm{U}} + \mathcal{C}_{\mathrm{D2D}}^{\mathrm{U}}} = \frac{(1-P_{\mathrm{OL}})R_{\mathrm{C}} + P_{\mathrm{OL}}R_{\mathrm{D2D}}}{W\left(X^{\mathrm{U}} + Y^{\mathrm{U}}\right)}, \quad (25)$$

where

$$X^{\mathrm{U}} = \frac{1}{\lambda_{\mathrm{U}}}\left(a_{\mathrm{E}}P_{\mathrm{BS}}^{\mathrm{U}} + P_{\mathrm{OM}}\right)\lambda_{\mathrm{B}}, \quad (26)$$

$$Y^{\mathrm{U}} = \frac{1}{\lambda_{\mathrm{U}}}b_{\mathrm{E}}\lambda_{\mathrm{DT}}^{\mathrm{act}}P_{\mathrm{D_a}}^{\mathrm{U}}. \quad (27)$$

Proposition 6: For the large-scale D2D-enabled cellular network operating in the O mode with the total bandwidth in cellular tier $(1-\omega)W$, the cellular and D2D spatially average user rates of R_{C} and R_{D2D}, respectively, as well as having a BS density of λ_{B}, a mobile-traffic intensity of λ_{U}, a DT density λ_{DT} with the D2D offloading radius ϖ_{D}, the BS static operation power consumption P_{OM}, and the BS and DT power amplifier efficiencies of a_{E} and b_{E}, respectively, the network's ESE is expressed as

$$\eta_{\mathrm{ESE}}^{\mathrm{O}} = \frac{\mathcal{S}}{\mathcal{C}_{\mathrm{BS}}^{\mathrm{O}} + \mathcal{C}_{\mathrm{D2D}}^{\mathrm{O}}} = \frac{(1-P_{\mathrm{OL}})R_{\mathrm{C}} + P_{\mathrm{OL}}R_{\mathrm{D2D}}}{W\left(X^{\mathrm{O}} + Y^{\mathrm{O}}\right)}, \quad (28)$$

[5]According to [37], reception generally consumes less power than transmission.

where

$$X^{\mathrm{O}} = \frac{1}{\lambda_{\mathrm{U}}}\big(a_{\mathrm{E}} P_{\mathrm{BS}}^{\mathrm{O}} + P_{\mathrm{OM}}\big)\lambda_{\mathrm{B}}, \tag{29}$$

$$Y^{\mathrm{O}} = \frac{1}{\lambda_{\mathrm{U}}} b_{\mathrm{E}} \lambda_{\mathrm{DT}}^{\mathrm{act}} P_{\mathrm{D_a}}^{\mathrm{O}}. \tag{30}$$

IV. ESE Optimization for Mobile-Traffic-Aware D2D-Enabled Cellular Networks

In this section, we first evaluate the celluar user outage performance in large-scale mobile-traffic-aware D2D-enabled cellular networks for both U and O mods, and then propose a spectrum partitioning scheme for the O mode to maximize the achievable network's ESE under both the celluar-user outage constraint and D2D transmit power constraint.

A. Outage Performance

The outage performance of a typical BS-MD link with the coexist of D2D links is presented in the following two propositions for the U and O modes, respectively.

Proposition 7: In a large-scale D2D-enabled cellular network operating in the U mode, given an effective D2D transmission radius of ϖ_{D}, the outage probability for a typical BS-MD link is given by

$$Q_{\mathrm{U}} = 1 - \exp\left(-\left(\rho_1 + p_c \frac{\lambda_{\mathrm{DT}}^{\mathrm{act}}}{\lambda_{\mathrm{B}}}\rho_2\right)\right), \tag{31}$$

with $p_c = (P_{\mathrm{D}}/P_{\mathrm{C}})^{\frac{1}{\alpha}}$,

$$\rho_1 = \gamma^{\frac{2}{\alpha}} \int_{\gamma^{-\frac{2}{\alpha}}}^{+\infty} \frac{1}{1+u^{\frac{\alpha}{2}}}\, du, \tag{32}$$

$$\rho_2 = \gamma^{\frac{2}{\alpha}} \int_{\left(\sqrt{\pi\lambda_{\mathrm{B}}}\varpi_{\mathrm{D}}/p_c\gamma^{1/\alpha}\right)^2}^{+\infty} \frac{1}{1+u^{\frac{\alpha}{2}}}\, du, \tag{33}$$

$$\gamma = 2^{\frac{R_{\mathrm{C}}}{W_{\mathrm{C}}}} - 1. \tag{34}$$

Proof: See Appendix D. ∎

Utilizing $E[W_{\mathrm{C}}] = W\lambda_{\mathrm{B}}/\lambda_{\mathrm{U}}(1-P_{\mathrm{OL}})$, we define the average cellular outage probability in the U mode as

$$\widetilde{Q}_{\mathrm{U}}(\varpi_{\mathrm{D}}) = 1 - \exp\left(-\left(\widetilde{\rho}_1 + p_c \frac{\lambda_{\mathrm{DT}}^{\mathrm{act}}}{\lambda_{\mathrm{B}}}\widetilde{\rho}_2\right)\right), \tag{35}$$

where $\widetilde{\rho}_1$ and $\widetilde{\rho}_2$ are obtained respectively by replacing γ with $\widetilde{\gamma} = 2^{R_C\lambda_{\mathrm{U}}(1-P_{\mathrm{OL}})/W\lambda_{\mathrm{B}}} - 1$ in (33) and (34). The average cellular outage probability is a function of ϖ_{D} which is explicitly indicated in (35). Note that both $\widetilde{\rho}_1$ and $\widetilde{\rho}_2$ increase as $\widetilde{\gamma}$ increases, while $\widetilde{\gamma}$ is a monotonically decreasing function of ϖ_{D} since $(1-P_{\mathrm{OL}}) = \exp\big(-\pi\lambda_{\mathrm{DT}}\varpi_{\mathrm{D}}^2\big)$. This indicates that $\widetilde{Q}_{\mathrm{U}}(\varpi_{\mathrm{D}})$ is a a monotonically decreasing function of ϖ_{D}.

By setting $\rho_2 = 0$ in (31), we readily obtain the following result for the O mode.

Proposition 8: In a large-scale D2D-enabled cellular network operating in the O mode with the spectrum partitioning factor ω, given an effective D2D transmission radius of ϖ_{D}, the outage probability for a typical BS-MD link is given by

$$Q_{\mathrm{O}} = 1 - \exp\left(-\rho_1\right). \tag{36}$$

In the O mode, since $E[W_{\mathrm{C}}] = (1-\omega)W\lambda_{\mathrm{B}}/\lambda_{\mathrm{U}}(1-P_{\mathrm{OL}})$, we define the average cellular outage probability as

$$\widetilde{Q}_{\mathrm{O}}(\omega, \varpi_{\mathrm{D}}) = 1 - \exp\left(-\widetilde{\rho}_1'\right), \tag{37}$$

where

$$\widetilde{\rho}_1' = \widetilde{\gamma}'^{\frac{2}{\alpha}} \int_{\widetilde{\gamma}'^{-\frac{2}{\alpha}}}^{+\infty} \frac{1}{1+u^{\frac{\alpha}{2}}}\, du, \tag{38}$$

with $\widetilde{\gamma}' = 2^{R_C\lambda_{\mathrm{U}}(1-P_{\mathrm{OL}})/(1-\omega)W\lambda_{\mathrm{B}}} - 1$. Clearly, $\widetilde{Q}_{\mathrm{O}}$ is a monotonically increasing function of ω, and it is a monotonically decreasing function of ϖ_{D}. When investigating the influence of the spectral partitioning factor ω for given ϖ_{D}, we will simply denote the average cellular outage probability in the O mode as $\widetilde{Q}_{\mathrm{O}}(\omega)$.

B. Optimal Cross-Tier Spectrum Partitioning in O Mode

For the O model, the system bandwidth is partitioned orthogonally into the two segments of $(1-\omega)W$ and ωW for the cellular and D2D tiers, respectively. We propose a cross-tier spectrum partitioning scheme in the O mode to maximize the achievable network's ESE under both the cellular-user outage constraint and D2D transmit power constraint. Mathematically, this optimal spectrum partitioning can be formulated as the following optimization problem

$$\begin{aligned} \bar{\omega}^{\star} = \arg \max_{0<\omega<1} \ & \eta_{\mathrm{ESE}}^{\mathrm{O}}, \\ \text{s.t.} \ & \widetilde{Q}_{\mathrm{O}}(\omega) < \theta_{\mathrm{O}}, \\ & P_{\mathrm{D_a}}^{\mathrm{O}}(\omega) < \mathrm{Z}_{\mathrm{O}}^{\mathrm{D}}, \end{aligned} \tag{39}$$

where θ_{O} is the cellular user outage threshold, and we have explicitly indicated that the average D2D transmit power $P_{\mathrm{D_a}}^{\mathrm{O}}$ is a function of ω.

Since increasing the spectrum portion of the D2D tier decreases the requirement of D2D transmit power, $P_{\mathrm{D_a}}^{\mathrm{O}}(\omega)$ is a monotonically decreasing function of ω. But $\widetilde{Q}_{\mathrm{O}}(\omega)$ is a monotonically increasing function of ω. Therefore, the constrained feasible region for ω that satisfies both the celluar-user outage constraint and D2D transmit power constraint is $\omega \in [\omega_{\mathrm{D_a}}, \omega_{\mathrm{out}}]$, where $\omega_{\mathrm{D_a}}$ and ω_{out} can be numerically obtained from the following two equations respectively

$$P_{\mathrm{D_a}}^{\mathrm{O}}\big(\omega_{\mathrm{D_a}}\big) = \mathrm{Z}_{\mathrm{O}}^{\mathrm{D}}, \tag{40}$$

$$\widetilde{Q}_{\mathrm{O}}\big(\omega_{\mathrm{out}}\big) = \theta_{\mathrm{O}}. \tag{41}$$

Clearly, if $\omega_{\mathrm{D_a}} > \omega_{\mathrm{out}}$, the feasible region of ω is empty, and there exists no solution for the constrained optimization (39).

Proposition 9: Given the effective D2D transmission range of ϖ_{D}, there exists an unique $\omega^{\star}$ that maximizes the network's ESE and it can be obtained numerically from (42)

$$\begin{aligned} &\frac{\omega^2 a_{\mathrm{E}} P_C\big(1-P_{\mathrm{OL}}\big) R_{\mathrm{C}} 2^{\frac{R_{\mathrm{C}}}{(1-\omega)W}}}{(1-\omega)^2 2^{\frac{\beta R_{\mathrm{D2D}}}{\omega W}} \pi b_{\mathrm{E}} \lambda_{\mathrm{DT}}^{\mathrm{act}} \mathcal{K} P_D P_{\mathrm{OL}} R_{\mathrm{D2D}}} \\ &= \left(1 - \frac{\lambda_{\mathrm{U}}\big(1-P_{\mathrm{OL}}\big)\Big(2^{\frac{R_{\mathrm{C}}}{(1-\omega)W}} - 1\Big)}{K\lambda_{\mathrm{B}}}\right)^{K+1} \\ &\quad \times \left(\frac{P_{\mathrm{OL}}}{\pi\lambda_{\mathrm{DT}}} - \frac{\varpi_{\mathrm{D}}^2}{\exp\big(\pi\lambda_{\mathrm{DT}}\varpi_{\mathrm{D}}^2\big)}\right). \end{aligned} \tag{42}$$

Proof: The derivative of $\eta_{\rm ESE}^{\rm OL}$ with respect to ω is

$$\frac{\partial \eta_{\rm ESE}^{\rm O}}{\partial \omega} = -\left(\frac{\partial X^{\rm O}}{\partial \omega} + \frac{\partial Y^{\rm O}}{\partial \omega}\right) \frac{(1-P_{\rm OL})\, R_{\rm C} + P_{\rm OL} R_{\rm D2D}}{W\left(X^{\rm O}+Y^{\rm O}\right)^2}, \tag{43}$$

in which

$$\frac{\partial X^{\rm O}}{\partial \omega} = \frac{\frac{2(\ln 2) a_{\rm E} P_C \left(1-P_{\rm OL}\right) R_{\rm C} 2^{\frac{R_{\rm C}}{(1-\omega)W}}}{(\alpha-2)(1-\omega)^2 W}}{\left(1 - \frac{\lambda_{\rm U}\left(1-P_{\rm OL}\right)\left(2^{\frac{R_{\rm C}}{(1-\omega)W}}-1\right)}{K\lambda_{\rm B}}\right)^{K+1}}, \tag{44}$$

$$\frac{\partial Y^{\rm O}}{\partial \omega} = \left(\frac{\varpi_{\rm D}^2}{\exp\left(\pi\lambda_{\rm DT}\varpi_{\rm D}^2\right)} - \frac{P_{\rm OL}}{\pi\lambda_{\rm DT}}\right) \times \frac{2(\ln 2)\pi b_{\rm E} 2^{\frac{\beta R_{\rm D2D}}{\omega W}} \lambda_{\rm DT}^{\rm act} \mathcal{K} P_D P_{\rm OL} R_{\rm D2D}}{(\alpha-2)\omega^2 W}. \tag{45}$$

Clearly, $\frac{\partial \eta_{\rm ESE}^{\rm O}}{\partial \omega} = 0$ is equivalent to $\frac{\partial X^{\rm O}}{\partial \omega} + \frac{\partial Y^{\rm O}}{\partial \omega} = 0$. Furthermore, it can be proved[6] that $\frac{\partial X^{\rm O}}{\partial \omega} \in [0, +\infty)$ is a monotonically increasing function of ω and $\frac{\partial Y^{\rm O}}{\partial \omega} \in [0, +\infty)$ is a monotonically decreasing function of ω since $\frac{\partial^2 X^{\rm O}}{\partial \omega^2} > 0$ and $\frac{\partial^2 Y^{\rm O}}{\partial \omega^2} < 0$. Therefore, there must exist a unique $\omega^\star$ which makes $\frac{\partial X^{\rm O}}{\partial \omega} + \frac{\partial Y^{\rm O}}{\partial \omega} = 0$. ■

We are ready to present the solution $\bar{\omega}^\star$.

Theorem 1: Let $\omega^\star$ be the unconstrained optimal spectrum partitioning solution obtained by solving (42). Assume that the feasible region of ω for the constrained optimization (39) is not empty, i.e., $\omega_{\rm D_a} \le \omega_{\rm out}$. Then the optimal solution $\bar{\omega}^\star$ for the constrained optimization (39) is given as follows.

Case 1. $\omega^\star < \omega_{\rm D_a}$: $\bar{\omega}^\star = \omega_{\rm D_a}$.

Case 2. $\omega_{\rm D_a} \le \omega^\star \le \omega_{\rm out}$: $\bar{\omega}^\star = \omega^\star$.

Case 3. $\omega^\star > \omega_{\rm out}$: $\bar{\omega}^\star = \omega_{\rm out}$.

V. Mobile-Traffic-Aware D2D-Enabled Offloading Performance Evaluation

We use numerical (theoretical) and simulation results to evaluate the ESE performance for a large-scale D2D-enabled cellular network. In particular, we investigate the influence of the key parameters, including the effective D2D transmission radius $\varpi_{\rm D}$ and the number of subbands in the D2D tier β, on the achievable network's ESE. Unless otherwise stated, the network has the total bandwidth $W = 20\,$MHz, the maximum BS transmit power $P_C = 20\,$watts, the maximum DT transmit power $P_D = 1\,$watt, the BS static power consumption $P_{\rm OM} = 20\,$watts, the BS and DT power amplifier efficiencies $a_{\rm E} = b_{\rm E} = 1$, and the DT density $\lambda_{\rm DT} = 150\,{\rm DTs/km}^2$. The pathloss exponent is set to $\alpha = 3.8$. The default network parameters are listed in Table II.

A. Impact of D2D Transmission Radius

The D2D transmission radius $\varpi_{\rm D}$ is one of the most important network parameters that influence the achievable network's ESE. The network's ESE performance in the U and O modes, $\eta_{\rm ESE}^{\rm U}$ and $\eta_{\rm ESE}^{\rm O}$, are depicted in Figs. 2 and 3, respectively, by varying $\varpi_{\rm D}$ as well as given various values of the mobile-traffic intensity $\lambda_{\rm U}$, where the BS density

[6]The proofs of $\frac{\partial^2 X^{\rm O}}{\partial \omega^2} > 0$ and $\frac{\partial^2 Y^{\rm O}}{\partial \omega^2} < 0$ are not difficult but are too tedious and hence are omitted here.

TABLE II
Default Network Parameters

parameter	value
$\lambda_{\rm B}$	$5\,{\rm BSs/km}^2$
$\lambda_{\rm DT}$	$150\,{\rm DTs/km}^2$
$\lambda_{\rm U}$	$200\,{\rm MDs/km}^2$
$\varpi_{\rm D}$	60 m
β	20
W	20 MHz
$R_{\rm C}$	0.2 Mb/s
$R_{\rm D2D}$	2 Mb/s
P_C	20 watts
$P_{\rm OM}$	20 watts
P_D	1 watts
$a_{\rm E} = b_{\rm E}$	1
α	3.8

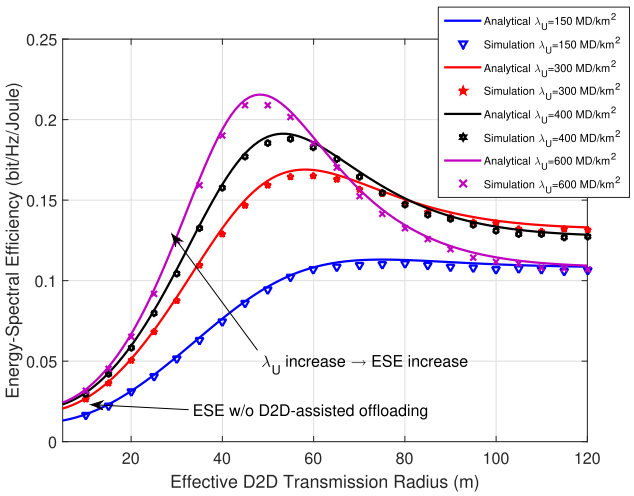

Fig. 2. Achievable network ESE performance (curve: analytical and point: simulation) in U mode by varying $\varpi_{\rm D}$ and $\lambda_{\rm U}$, given $\lambda_{\rm B} = 5\,{\rm BSs/km}^2$, $R_{\rm C} = 0.2\,{\rm Mb/s}$, $R_{\rm D2D} = 2\,{\rm Mb/s}$ and $\beta = 20$.

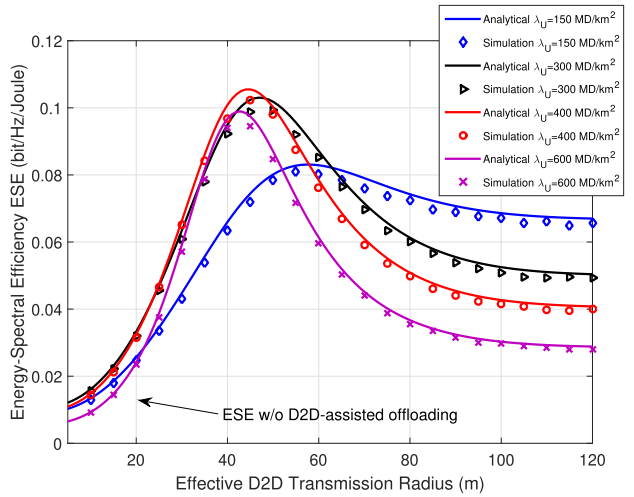

Fig. 3. Achievable network ESE performance (curve: analytical and point: simulation) in O mode by varying $\varpi_{\rm D}$ and $\lambda_{\rm U}$, given $\omega = 0.3$, $\lambda_{\rm B} = 5\,{\rm BSs/km}^2$, $R_{\rm C} = 0.2\,{\rm Mb/s}$, $R_{\rm D2D} = 2\,{\rm Mb/s}$ and $\beta = 20$.

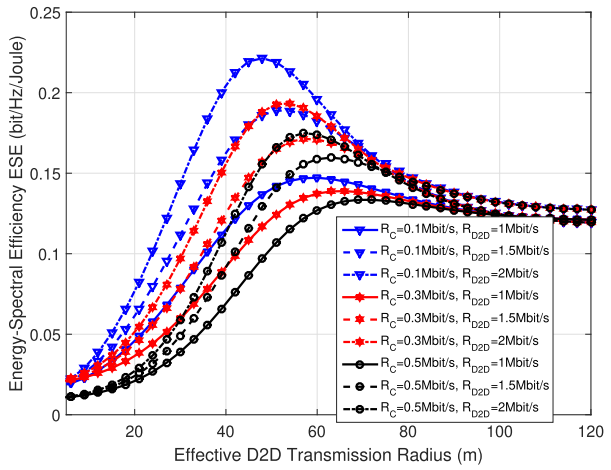

Fig. 4. Achievable network ESE performance in U mode by varying ϖ_{D} as well as R_{C} and R_{D2D}, given $\lambda_{\mathrm{U}} = 500\,\mathrm{MDs/km}^2$, $\lambda_{\mathrm{B}} = 5\,\mathrm{BSs/km}^2$ and $\beta = 20$.

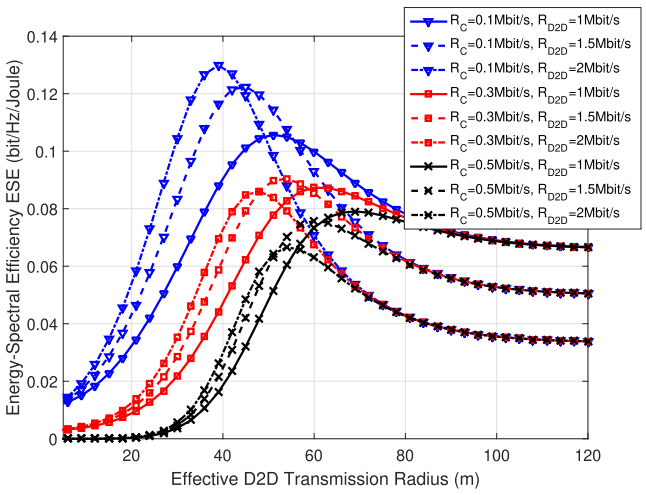

Fig. 5. Achievable network ESE performance in O mode by varying ϖ_{D} as well as R_{C} and R_{D2D}, given $\omega = 0.5$, $\lambda_{\mathrm{U}} = 500\,\mathrm{MDs/km}^2$, $\lambda_{\mathrm{B}} = 5\,\mathrm{BSs/km}^2$ and $\beta = 20$.

$\lambda_{\mathrm{B}} = 5\,\mathrm{BSs/km}^2$, the average cellular service rate $R_{\mathrm{C}} = 0.2\,\mathrm{Mb/s}$, the average D2D service rate $R_{\mathrm{D2D}} = 2\,\mathrm{Mb/s}$, and $\beta = 20$, while additionally for the O mode network, the D2D-tier bandwidth fraction $\omega = 0.3$. Note that $\varpi_{\mathrm{D}} \to 0$ corresponds to the network without D2D-enable offloading, which is indicated by 'ESE w/o D2D-assisted offloading' in Figs. 2 and 3. It can be seen that the analytical values and the simulated results of the network's ESE agree with each other well. This verifies the accuracy of our theoretical ESE modeling. Observe from both Figs. 2 and 3 that the network's ESE increases quite fast with ϖ_{D} when ϖ_{D} is relatively small, and after reaching the peak value, the network's ESE becomes decreasing as ϖ_{D} increases. Also the network's ESE becomes saturated for sufficiently large ϖ_{D}. This is because when the effective D2D transmission radius is large, most of the cellular mobile-traffic have been offloaded to the D2D tier, and enlarging further ϖ_{D} will not alter the achievable ESE noticeably. It can also be seen from Fig. 2 that for relatively small ϖ_{D}, increasing the mobile-traffic intensity λ_{U} always leads to a higher $\eta_{\mathrm{ESE}}^{\mathrm{U}}$ but the same cannot be said for relatively large ϖ_{D}. As for the O mode network, the influence of λ_{U} to $\eta_{\mathrm{ESE}}^{\mathrm{O}}$ is more complicated, which also depends on ϖ_{D}. Observe from Fig. 3 that for relatively large ϖ_{D}, increasing λ_{U} always leads to the decrease in $\eta_{\mathrm{ESE}}^{\mathrm{O}}$.

We continue to investigate the impacts of the effective D2D transmission radius ϖ_{D} as well as the cellular and D2D links' service data rates R_{C} and R_{D2D} by varying ϖ_{D} as well as R_{C} and R_{D2D}, and the resulting networks' ESE performance in the U and O modes are depicted in Figs. 4 and 5, respectively, where $\lambda_{\mathrm{U}} = 500\,\mathrm{MDs/km}^2$, $\lambda_{\mathrm{B}} = 5\,\mathrm{BSs/km}^2$ and β=20, while additionally for the O mode network, $\omega = 0.5$. Obviously, the influence of ϖ_{D} to the network's ESE is similar to that depicted in Figs. 2 and 3. We note that for the relatively small ϖ_{D}, the increase of the D2D tier service rate R_{D2D} leads to the increase of the network's ESE but by contrast, increasing the cellular service rate R_{C} causes the decrease in the network's ESE. This implies that the cellular link is not an energy-spectral efficient link, in comparison with the D2D link, owing to its large distance and scarce spectrum resources.

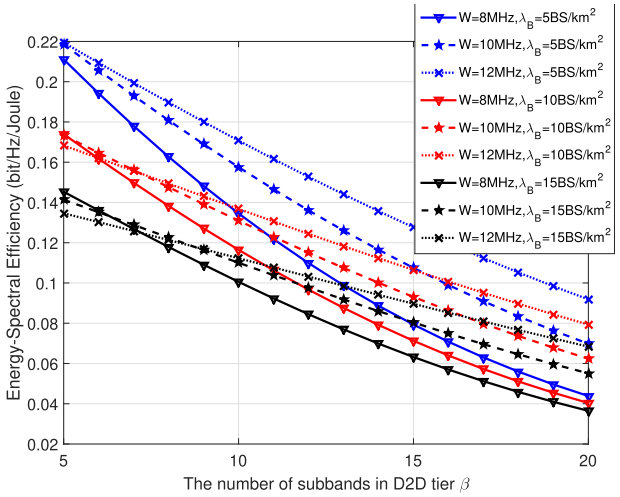

Fig. 6. Achievable network ESE performance in U mode by varying β as well as W and λ_{B}, given $R_{\mathrm{C}} = 0.3\,\mathrm{Mb/s}$, $R_{\mathrm{D2D}} = 2\,\mathrm{Mb/s}$ and $\lambda_{\mathrm{U}} = 500\,\mathrm{MDs/km}^2$.

An interesting phenomenon observed from Figs. 4 and 5 is that for the same D2D-link service rate R_{D2D}, the ESEs corresponding to different cellular service rates R_{C} approach to a same value when ϖ_{D} is large. This is easy to understand since most of the mobile-traffic have been offloaded to the D2D tier for large ϖ_{D} and the network's ESE is mainly determined by R_{D2D}.

B. Impact of D2D Access Probability

The D2D access probability $1/\beta$ or the number of sub-bands in the D2D tier β is another key network parameter that significantly influences the network's achievable ESE performance. The achievable $\eta_{\mathrm{ESE}}^{\mathrm{U}}$ and $\eta_{\mathrm{ESE}}^{\mathrm{O}}$ are depicted in Figs. 6 and 7, respectively, by varying β as well as W and λ_{B}, where $R_{\mathrm{C}} = 0.3\,\mathrm{Mb/s}$, $R_{\mathrm{D2D}} = 2\,\mathrm{Mb/s}$ and $\lambda_{\mathrm{U}} = 500\,\mathrm{MDs/km}^2$, while additionally for the O-mode network, $\omega = 0.5$. As expected, increasing the BS density λ_{B}

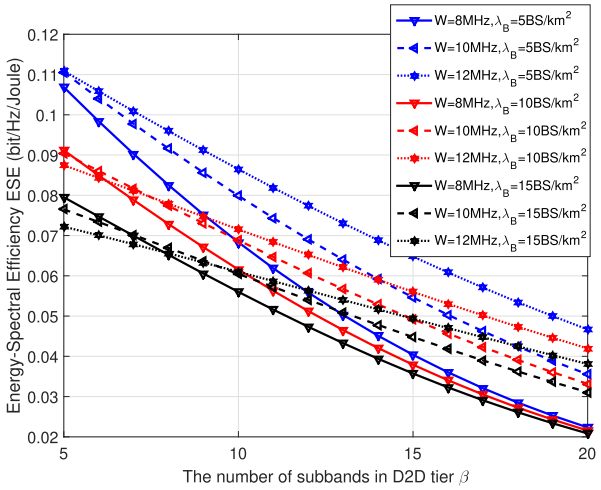

Fig. 7. Achievable network ESE performance in O mode by varying β as well as W and λ_{B}, given $\omega = 0.5$, $R_{\mathrm{C}} = 0.3\,\mathrm{Mb/s}$, $R_{\mathrm{D2D}} = 2\,\mathrm{Mb/s}$ and $\lambda_{\mathrm{U}} = 500\,\mathrm{MDs/km^2}$.

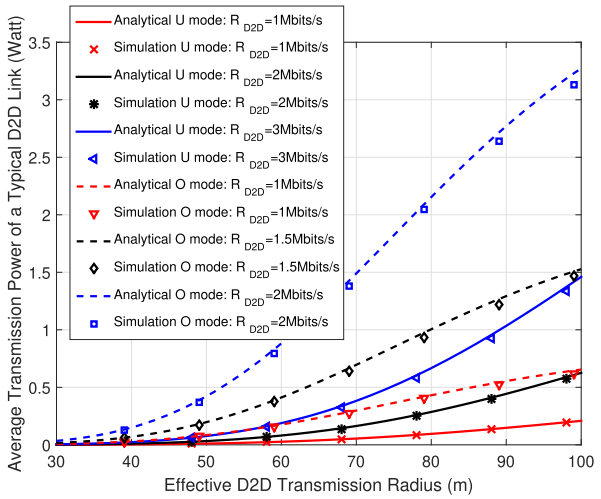

Fig. 8. Average required D2D transmit power (curve: analytical and point: simulation) as the function of ϖ_{D} and R_{D2D}, given $\lambda_{\mathrm{U}} = 500\,\mathrm{MDs/km^2}$, $R_{\mathrm{C}} = 0.2\,\mathrm{Mb/s}$, $\lambda_{\mathrm{B}} = 5\,\mathrm{BSs/km^2}$ and $\beta = 20$, while $\omega = 0.5$ for the O-mode network.

decreases the achievable ESE in general, since the increased interference as a result of increasing λ_{B} outweighs the effect of the reduced BS-MD distance. It can be seen that the network's ESE is a monotonically decreasing function of β. As expected, given $\lambda_{\mathrm{B}} = 5\,\mathrm{BS/km^2}$, increasing the system bandwidth W increases the achievable network's ESE, while given $\lambda_{\mathrm{B}} = 10\,\mathrm{BS/km^2}$ and $15\,\mathrm{BS/km^2}$ as well as for not too small β, the network's ESE is an increasing function of W. Also observe that $\eta_{\mathrm{ESE}}^{\mathrm{O}}$ is smaller than $\eta_{\mathrm{ESE}}^{\mathrm{U}}$ in general, suggesting that the underlay operating mode is more spectrum and energy efficient than the overlay operating mode.

C. Performance Evaluation

Fig. 8 quantifies the required average D2D transmit powers of a typical D2D link in both the U and O modes, $P_{\mathrm{D_a}}^{\mathrm{U}}$ and $P_{\mathrm{D_a}}^{\mathrm{O}}$, as the functions of R_{D} and R_{D2D}, given $R_{\mathrm{C}} = 0.2\,\mathrm{Mb/s}$, $\lambda_{\mathrm{U}} = 500\,\mathrm{MDs/km^2}$, $\lambda_{\mathrm{B}} = 5\,\mathrm{BSs/km^2}$ and $\beta = 20$, while additionally $\omega = 0.5$ for the O-mode network. In Fig. 8, curves are the theoretical $P_{\mathrm{D_a}}^{\mathrm{U}}$ and $P_{\mathrm{D_a}}^{\mathrm{O}}$ calculated according to Propositions 1 and 2, while points correspond to the simulated results. Clearly, the simulated results agree with the analytical values well. In line with Propositions 1 and 2, the average D2D transmit power increases monotonically with ϖ_{D}. Obviously, $P_{\mathrm{D_a}}^{\mathrm{U}}$ is smaller than $P_{\mathrm{D_a}}^{\mathrm{O}}$ as more spectrum resource is available to D2D links in the U mode, and the increase of the mobile-traffic intensity increases the required average D2D transmit power as expected.

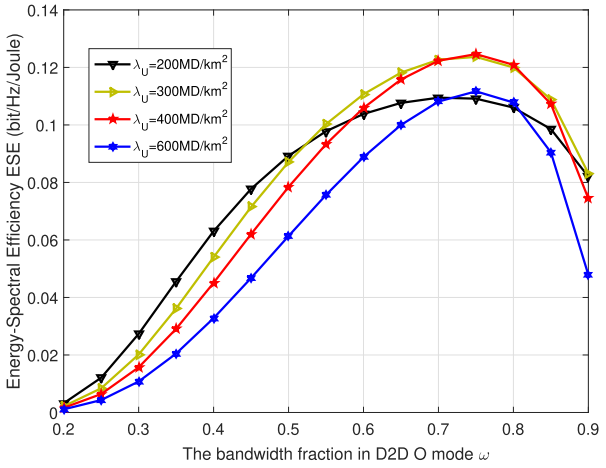

Fig. 9. Achievable network's ESE in O mode as the function of ω and λ_{U}, given $\varpi_{\mathrm{D}} = 60\,\mathrm{m}$, $R_{\mathrm{C}} = 0.2\,\mathrm{Mb/s}$, $R_{\mathrm{D2D}} = 2\,\mathrm{Mb/s}$, $\lambda_{\mathrm{B}} = 5\,\mathrm{BS/km^2}$ and $\beta = 20$.

TABLE III
OPTIMAL SPECTRUM SHARING SOLUTION FOR THE O-MODE NETWORK UNDER CELLULAR USER OUTAGE PERFORMANCE AND D2D TRANSMITTER POWER CONSTRAINTS

θ_{O}	$Z_{\mathrm{O}}^{\mathrm{D}}$	$[\omega_{\mathrm{D_a}},\ \omega_{\mathrm{out}}]$	$\bar{\omega}^{\star}$
0.21	0.12	[0.75, 0.80]	0.75
0.18	0.32	[0.60, 0.75]	0.70
0.10	1.70	[0.40, 0.55]	0.55
0.12	0.09	$\omega_{\mathrm{D_a}} = 0.80 > \omega_{\mathrm{out}} = 0.60$	no solution

In Fig. 9, the relationship between the O-mode network's ESE $\eta_{\mathrm{ESE}}^{\mathrm{O}}$ and the fraction of the total bandwidth ω is illustrated. In line with Proposition 9, there exists a unique unconstrained optimal $\omega^{\star}$, which maximizes the achievable network's ESE $\eta_{\mathrm{ESE}}^{\mathrm{O}}$. Furthermore, increasing the mobile-traffic intensity moves the optimal $\omega^{\star}$ to the right, which implies that when λ_{U} is increased, we need allocate more spectrum to the D2D tier in order to attain a higher ESE.

D. Optimal Spectrum Partitioning in O Mode

We now illustrate our optimal spectrum sharing design of the constrained optimization (39) for the large-scale D2D-enabled cellular network operating in the O mode. The network parameters are given in Table II. For this network, the optimal unconstrained spectrum partitioning solution that maximizes the network's ESE $\eta_{\mathrm{ESE}}^{\mathrm{O}}$ is $\omega^{\star} = 0.70$, which can be obtained by solving (42). From Fig. 9, it can also be seen that $\omega^{\star} = 0.70$ corresponds to the peak value of the

$\eta_{\rm ESE}^{\rm O}$ curve related to $\lambda_{\rm U} = 200\,{\rm MDs/km}^2$ as to be expected. The optimal constrained solutions $\bar{\omega}^\star$ obtained according to Theorem 1 are listed in Table III given different values of the cellular outage threshold $\theta_{\rm O}$ and D2D transmit power capacity $Z_{\rm O}^{\rm D}$.

VI. Conclusions

Based on the practical D2D-assisted offloading protocol conceived for the future 5G cellular network, we have proposed an ESE evaluation framework for large-scale mobile-traffic-aware D2D-enabled cellular networks operating in U and O modes, respectively, which allows us to analyze the impact of user-behaviors, D2D-assisted offloading parameters and cellular network operating conditions on the achievable network's ESE. Since all the our analytical results have been derived in closed-form and their accuracy has been verified in an extensive simulation study, they provide efficient and practical tools for designing and evaluating future D2D enabled cellular networks. With aid of our tractable and efficient ESE analytical tool, we have further designed an optimal spectrum partitioning scheme for large-scaled D2D-enabled cellular networks operating in O mode to maximize the network's ESE with cellular user outage performance and D2D transmitters' power as constraints. This solution/design is particularly valuable to future D2D enabled cellular networks operating in O mode, because it ensures that the optimal offloading strategy always matches both the users behaviors and cellular operation conditions.

Appendix

A. Proof of Proposition 1

Proof: Recall that a typical MD u_i has the offloading region $\mathbb{O}\big(u_i, \varpi_{\rm D}\big)$. A typical activated DT by broadcasting can simultaneously serve one or more MDs who's distances to the DT are less than or equal to $\varpi_{\rm D}$. Let $\lambda_{\rm DT}^{\rm act}$ denote the density of active DTs, which can be expressed as

$$\lambda_{\rm DT}^{\rm act} = \frac{\Pr\big(N_{\mathbb{O}_{u_i}} \geq 1\big)\lambda_{\rm U}}{E[N_{\rm DT}]}, \tag{46}$$

where $E[N_{\rm DT}]$ is the average number of MDs served by a DT. Let d denote the distance between u_i and its nearest DT. Then the probability density function (PDF) of d is given by $f(d) = 2\pi\lambda_{\rm DT}\exp\big(-\pi\lambda_{\rm DT}d^2\big)$. Therefore, the probability for a typical MD u_i is offloaded by DTs can be expressed as

$$\begin{aligned} P_{\rm OL} &= \Pr\big(N_{\mathbb{O}_{u_i}} \geq 1\big) = \int_0^{\varpi_{\rm D}} f(x)\,dx \\ &= 1 - \exp\big(-\pi\lambda_{\rm DT}\varpi_{\rm D}^2\big). \end{aligned} \tag{47}$$

Since the MDs are distributed according to a PPP, the probability massive function (PMF) of $N_{\rm DT}$ is $f_{\rm DT}(N_{\rm DT}) = \big(\pi\lambda_{\rm U}\varpi_{\rm D}^2\big)^{N_{\rm DT}}\exp\big(-\pi\lambda_{\rm U}\varpi_{\rm D}^2\big)/\big(N_{\rm DT}!\big)$, e.g., [38], where $\pi\lambda_{\rm U}\varpi_{\rm D}^2$ is the circular area covered by a typical DT. Therefore, the density of active DTs can be expressed as

$$\lambda_{\rm DT}^{\rm act} = \sum_{N_{\rm DT}=1}^{+\infty} \frac{\big(\pi\lambda_{\rm U}\varpi_{\rm D}^2\big)^{N_{\rm DT}}\lambda_{\rm U}P_{\rm OL}}{N_{\rm DT}\exp\big(\pi\lambda_{\rm U}\varpi_{\rm D}^2\big)\big(N_{\rm DT}\big)}. \tag{48}$$

By applying the well-known property of the infinite series (48) and using the notation $y = \pi\lambda_{\rm U}\varpi_{\rm D}^2$, $\lambda_{\rm DT}^{\rm act}$ can be obtained as

$$\begin{aligned} \lambda_{\rm DT}^{\rm act} &= \big({\rm Ei}(y) - {\rm Ei}(1) - \ln y + 1.3179\big)\exp(-y)P_{\rm OL}\lambda_{\rm U} \\ &= \mathcal{K}P_{\rm OL}\lambda_{\rm U}, \end{aligned} \tag{49}$$

where ${\rm Ei}(y) = -\int_{-y}^{\infty}\frac{\exp(-t)}{t}\,dt$.

From (6), the average transmit power for the typical D2D link associated with the MD $u_k^{D,j}$ in the U mode is given by

$$P_{\rm D_a}^{\rm U} = E\left[\frac{\Big(2^{\frac{\beta R_{\rm D2D}}{W}} - 1\Big)}{l_k^{D,n}h_k^{D,n}}\big(I_n^{CD} + I_n^{DD}\big)\right], \tag{50}$$

where the expectation $E[\cdot]$ is with respect to the distribution of the interferers' layout and the links' channel gains related to the links between the typical MD $u_k^{D,j}$ and its associated DTs [28]. Let $\mathcal{M}_{I_n^{CD}}(s)$ and $\mathcal{M}_{I_n^{DD}}(s)$ be the moment-generating functions (MGFs) of I_n^{CD} and I_n^{DD}, respectively. According to [39] as well as the well-known property of MGFs $x = -\frac{\partial}{\partial s}\ln\mathcal{M}_x(s)\big|_{s=0}$, (50) can be expressed as

$$P_{\rm D_a}^{\rm U} = \frac{2^{\frac{\beta R_{\rm D2D}}{W}} - 1}{r_{\rm dd}^{-\alpha}}\left(-\frac{\partial}{\partial s}\ln\mathcal{M}_{I_n^{CD}} - \frac{\partial}{\partial s}\ln\mathcal{M}_{I_n^{DD}}\right)\Big|_{s=0}, \tag{51}$$

where

$$r_{\rm dd} = \min_n \big\|u_k^{D,j} - {\rm DT}_n\big\| \leq \varpi_{\rm D}. \tag{52}$$

Next consider the D2D tier interference $I'_{\rm dd}$ contributed by the PPP distributed DT interferers in the finite annular region with the inner diameter $r_{\rm dd}$ and the outer diameter $r_{\rm out,D}$. The MGF of $I'_{\rm dd}$ is given by

$$\mathcal{M}_{I'_{\rm dd}}(s) = \exp\left(2\pi\lambda_{\rm DT}^{\rm act}\int_{r_{\rm dd}}^{r_{\rm out,D}}\left(1 - \exp\big(-\frac{sP_D}{\beta y^\alpha}\big)\right)y\,dy\right). \tag{53}$$

Similarly, consider the cellular tier interference $I'_{\rm cd}$ contributed by the PPP distributed BS interferers in the finite annular region with the inner diameter $r_{\rm cd}$, where

$$r_{\rm cd} = \min_{l\in\Theta_{\rm B}}\big\|u_k^{D,j} - b_l\big\|, \tag{54}$$

and the outer diameter $r_{\rm out,C}$. The MGF of $I'_{\rm cd}$ is given by

$$\mathcal{M}_{I'_{\rm cd}}(s) = \exp\left(2\pi\lambda_{\rm B}\int_{r_{\rm cd}}^{r_{\rm out,C}}\left(1 - \exp\big(-\frac{sP_C}{\beta x^\alpha}\big)\right)x\,dx\right). \tag{55}$$

Thus

$$I'_{\rm dd} = -\frac{\partial\ln\mathcal{M}_{I'_{\rm dd}}(s)}{\partial s}\Big|_{s=0} = \frac{2\pi\lambda_{\rm DT}^{\rm act}P_D\big(r_{\rm out,D}^{2-\alpha} - r_{\rm dd}^{2-\alpha}\big)}{(2-\alpha)\beta}, \tag{56}$$

$$I'_{\rm cd} = -\frac{\partial\ln\mathcal{M}_{I'_{\rm cd}}(s)}{\partial s}\Big|_{s=0} = \frac{2\pi\lambda_{\rm B}P_C\big(r_{\rm out,C}^{2-\alpha} - r_{\rm cd}^{2-\alpha}\big)}{(2-\alpha)\beta}. \tag{57}$$

Clearly,

$$\lim_{r_{\rm out,D}\to\infty} I'_{\rm dd} = I_n^{DD}, \tag{58}$$

$$\lim_{r_{\rm out,C}\to\infty} I'_{\rm cd} = I_n^{CD}. \tag{59}$$

For $\alpha > 2$, plugging (56) to (59) into (51) yields the typical D2D link's average transmit power conditioned on $r_{\rm cd}$ and $r_{\rm dd}$ as

$$P_{\rm D_a}^{\rm U}\Big|_{r_{\rm cd},r_{\rm dd}} = \frac{2\pi\left(2^{\frac{\beta R_{\rm D2D}}{W}}-1\right)}{\beta(\alpha-2)}\Big(\lambda_{\rm B}P_C r_{\rm cd}^{2-\alpha}r_{\rm dd}^{\alpha} + \mathcal{K}P_{\rm OL}\lambda_{\rm U}P_D r_{\rm dd}^2\Big). \quad (60)$$

Further denote $v = r_{\rm cd}$ and $u = r_{\rm dd}$. By integrating (60) with the PDFs of u and v, we obtain the average transmit power $P_{\rm D_a}^{\rm U}$ given by

$$P_{\rm D_a}^{\rm U} = \frac{8\pi^3\left(2^{\frac{\beta R_{\rm D2D}}{W}}-1\right)}{\beta(\alpha-2)}\int_0^{\varpi_{\rm D}}\frac{\lambda_{\rm DT}u^{\alpha+1}}{\exp(\pi\lambda_{\rm DT}u^2)} \times\int_0^{+\infty}\left(\frac{\lambda_{\rm B}^2P_C v^{3-\alpha}}{\exp(\pi\lambda_{\rm B}v^2)}+\frac{P_D\lambda_{\rm B}\mathcal{K}\lambda_{\rm U}u^{2-\alpha}v}{\exp(\pi\lambda_{\rm B}v^2)}P_{\rm OL}\right)dv\,du. \quad (61)$$

After some algebraic manipulations to complete the integration (61), we obtain the expression of $P_{\rm D_a}^{\rm U}$ which is the righthand side of the inequality (10). This completes the proof. ■

B. Proof of Proposition 2

Proof: The average transmit power for the typical D2D link associated with the MD $u_k^{D,j}$ in the O mode is given by

$$P_{\rm D_a}^{\rm O} = E\left[\frac{\left(2^{\frac{\beta R_{\rm D2D}}{\omega W}}-1\right)I_n^{DD}}{l_k^{D,n}h_k^{D,n}}\right], \quad (62)$$

which is obtained by removing I_n^{CD} and replacing W with ωW in (50). Similar to the derivation of (60), by considering the interfer layout $\overline{\mathbb{O}}\big(u_k^{D,j}, r_{\rm dd}\big)$ with $r_{\rm dd}$ as given in (52), the average D2D transmit power in the O mode conditioned on $r_{\rm dd}$ can be expressed as

$$P_{\rm D_a}^{\rm O}\Big|_{r_{\rm dd}} = \left(2^{\frac{\beta R_{\rm D2D}}{\omega W}}-1\right)\frac{2\pi\mathcal{K}\lambda_{\rm U}P_D r_{\rm dd}^2P_{\rm OL}}{\beta(\alpha-2)}. \quad (63)$$

Again denote $u = r_{\rm dd}$. By integrating (63) with the PDF of u, we arrive at

$$P_{\rm D_a}^{\rm O} = \int_0^{\varpi_{\rm D}}\left(2^{\frac{\beta R{\rm D2D}}{\omega W}}-1\right)\frac{4\pi^2\mathcal{K}P_D u^3}{\beta(\alpha-2)} \times P_{\rm OL}\lambda_{\rm U}\lambda_{\rm DT}\exp\left(-\pi\lambda_{\rm DT}u^2\right)du. \quad (64)$$

After some algebraic manipulations to complete the integration (64), we obtain the expression of $P_{\rm D_a}^{\rm O}$ which is the righthand side of the inequality (15). This completes the proof. ■

C. Proof of Proposition 3

Proof: From (2), the average required transmit power for the typical link between BS b_j and MD $u_i^{C,j}$ in the U mode can be expressed by

$$P_{{\rm C},i}^{\rm U} = E\left[\frac{\left(2^{\frac{R_{\rm C}}{W_C}}-1\right)\left(I_j^{CC}+I_j^{DC}\right)}{l_i^{C,j}h_i^{C,j}}\right], \quad (65)$$

where the interference I_j^{CC} and I_j^{DC} are given in (3) and (4), respectively, and hence the cellular and D2D interfer layouts, $\Theta_B\backslash b_j$ and $\overline{\mathbb{O}}\big(u_i^{C,j},\varpi_{\rm D}\big)$, are conditioned with $r_{\rm cc} = \|u_i^{C,j} - b_j\|$. With the aid of the MGFs for I_j^{CC} and I_j^{DC}, we have

$$P_{{\rm C},i}^{\rm U} = \left(2^{\frac{R_{\rm C}}{W_C}}-1\right)r_{\rm cc}^{\alpha}\left(-\frac{\partial\ln\mathcal{M}_{I_j^{CC}}}{\partial s}-\frac{\partial\ln\mathcal{M}_{I_j^{DC}}}{\partial s}\right)\Big|_{s=0}. \quad (66)$$

Similar to the proof of Proposition 1, define the cellular tier interference $I'_{\rm cc}$ in the corresponding annular region and the D2D tier interference $I'_{\rm dc}$ in the relavent annular region. Then their MGFs are given respectively by

$$\mathcal{M}_{I'_{\rm cc}} = \exp\left(2\pi\lambda_{\rm B}\int_{r_{\rm cc}}^{r_{\rm bn,C}}\left(1-\exp\left(-\frac{sP_C}{N_C x^{\alpha}}\right)\right)x\,dx\right), \quad (67)$$

$$\mathcal{M}_{I'_{\rm dc}} = \exp\left(2\pi\lambda_{\rm DT}^{\rm act}\int_{\varpi_{\rm D}}^{r_{\rm bn,D}}\left(1-\exp\left(-\frac{sP_D}{N_C x^{\alpha}}\right)\right)x\,dx\right). \quad (68)$$

Based on the well-known property of MGFs, we have

$$-\frac{\partial\ln\mathcal{M}_{I'_{\rm cc}}}{\partial s}\Big|_{s=0} = \frac{2\pi\lambda_{\rm B}P_C\left(r_{\rm bn,C}^{2-\alpha}-r_{\rm cc}^{2-\alpha}\right)}{(2-\alpha)N_C}, \quad (69)$$

$$-\frac{\partial\ln\mathcal{M}_{I'_{\rm dc}}}{\partial s}\Big|_{s=0} = \frac{2\pi\lambda_{\rm DT}^{\rm act}P_D\left(r_{\rm bn,D}^{2-\alpha}-\varpi_{\rm D}^{2-\alpha}\right)}{(2-\alpha)N_C}. \quad (70)$$

By taking $r_{\rm bn,C}\to\infty$ and $r_{\rm bn,D}\to\infty$ in (69) and (70), respectively, and plugging the results into (66), we obtain the average DL transmit power of a typical BS-MD link associated with $u_i^{C,j}$ and conditioned on $r_{\rm cc}$ as

$$P_{{\rm C},i}^{\rm U}\Big|_{r_{\rm cc}} = \frac{2\pi\left(2^{\frac{R_{\rm C}}{W_C}}-1\right)}{N_C(\alpha-2)}\Big(\lambda_{\rm B}P_C r_{\rm cc}^2 + \mathcal{K}P_{\rm OL}\lambda_{\rm U}P_D\varpi_{\rm D}^{2-\alpha}r_{\rm cc}^{\alpha}\Big). \quad (71)$$

Since the PDF of $r_{\rm cc}$ is $f\big(r_{\rm cc}\big) = 2\pi\lambda_{\rm B}r_{\rm cc}\exp\big(-\pi\lambda_{\rm B}r_{\rm cc}^2\big)$, the average required DL transmit power for $u_i^{C,j}$ is

$$P_{{\rm C},i}^{\rm U} = \int_0^{+\infty}P_{{\rm C},i}^{\rm U}\Big|_{r_{\rm cc}=x}f(x)\,dx. \quad (72)$$

Completing the integral (72) leads to the average DL transmit power given in (16).

Then, we focus on b_j having the coverage area of $S_{A,j} = S_A$ and serving $N_{\rm C}$ cellular MDs. Since the PMF of $N_{\rm C}\geq 1$ is given by [38]

$$g(N_{\rm C}) = \frac{\left((1-P_{\rm OL})\lambda_{\rm U}S_A\right)^{N_C}}{\left(N_C!\right)\exp\left((1-P_{\rm OL})\lambda_{\rm U}S_A\right)}, \quad (73)$$

and all the cellular MDs have the identical rate of $R_{\rm C}$, the average aggregate DL transmit power conditioned on the

cell size of S_A is given by

$$P_{\mathrm{BS}}^{\mathrm{U}}\Big|_{S_A} = \sum_{N_C=1}^{\infty}\sum_{i=1}^{N_C} g\left(N_C\right) P_{\mathrm{C},i}^{\mathrm{U}} = \frac{2}{\alpha-2}\left(P_C + \frac{\alpha\Gamma\left(\frac{\alpha}{2}\right)\pi^{\frac{2-\alpha}{2}} P_D \lambda_{\mathrm{U}} \mathcal{K} P_{\mathrm{OL}}}{2\lambda_{\mathrm{B}}^{\frac{\alpha}{2}} \varpi_{\mathrm{D}}^{\alpha-2}}\right) \times \left(\exp\left(\left(2^{\frac{R_{\mathrm{C}}}{W}}-1\right)\left(1-P_{\mathrm{OL}}\right)\lambda_{\mathrm{U}} S_A\right)-1\right). \tag{74}$$

Noting that the PDF of S_A is given by $f_{S_A}(t) = \lambda_{\mathrm{B}}^K \frac{K^K}{\Gamma(K)} t^{K-1} \exp\left(-K\lambda_{\mathrm{B}} t\right)$ with $K = 3.75$ [40], we have

$$P_{\mathrm{BS}}^{\mathrm{U}} = \int_0^{\infty} P_{\mathrm{BS}}^{\mathrm{U}}\Big|_{S_A=t} f_{S_A}(t)\, dt. \tag{75}$$

After some algebraic manipulations to complete the integral (75), we arrive at (17). This completes the proof. ∎

D. Proof of Proposition 7

Proof: The outage probability of a typical cellular user $u_i^{C,j}$ conditioned on r_{cc} is given by

$$Q_j^{C,i}\Big|_{r_{\mathrm{cc}}} = 1 - \exp\left(-2\pi\lambda_{\mathrm{B}}\int_{r_{\mathrm{cc}}}^{\infty} \frac{\gamma}{\gamma + \left(\frac{v}{r_{\mathrm{cc}}}\right)^{\alpha}} v\, dv\right) \times \exp\left(-2\pi\lambda_{\mathrm{DT}}^{\mathrm{act}} p_c \int_{p_c^{-1}\varpi_{\mathrm{D}}}^{\infty} \frac{\gamma}{\gamma + \left(\frac{v}{r_{\mathrm{cc}}}\right)^{\alpha}} v\, dv\right). \tag{76}$$

Considering the worst case that $u_i^{C,j}$ is at the cell edge, we have $r_{\mathrm{cc}} = \sqrt{1/\pi\lambda_{\mathrm{B}}}$, since $\pi r_{\mathrm{cc}}^2 = 1/\lambda_{\mathrm{B}}$. Plugging it into (76) and with the help of Appendix B of [35] completes the proof. ∎

REFERENCES

[1] L. Wei, R. Q. Hu, Y. Qian, and G. Wu, "Enable device-to-device communications underlaying cellular networks: Challenges and research aspects," *IEEE Commun. Mag.*, vol. 52, no. 6, pp. 90–96, Jun. 2014.

[2] A. Asadi, Q. Wang, and V. Mancuso, "A survey on device-to-device communication in cellular networks," *IEEE Commun. Surveys Tuts.*, vol. 16, no. 4, pp. 1801–1819, Nov. 2014.

[3] M. N. Tehrani, M. Uysal, and H. Yanikomeroglu, "Device-to-device communication in 5G cellular networks: Challenges, solutions, and future directions," *IEEE Commun. Mag.*, vol. 52, no. 5, pp. 86–92, May 2014.

[4] D. Astely, E. Dahlman, G. Fodor, S. Parkvall, and J. Sachs, "LTE release 12 and beyond," *IEEE Commun. Mag.*, vol. 51, no. 7, pp. 154–160, Jul. 2013.

[5] Y. Li, T. Wu, P. Hui, D. Jin, and S. Chen, "Social-aware D2D communications: Qualitative insights and quantitative analysis," *IEEE Commun. Mag.*, vol. 52, no. 6, pp. 150–158, Jun. 2014.

[6] (Feb. 7, 2017). *Cisco Visual Networking Index: Global Mobile Data Traffic Forecast Update, 2016–2021*. [Online]. Available: http://www.cisco.com/c/en/us/solutions/collateral/service-provider/visual-networking-index-vni/mobile-white-paper-c11-520862.html

[7] Y. Shen, C. Jiang, T. Q. S. Quek, and Y. Ren, "Device-to-device-assisted communications in cellular networks: An energy efficient approach in downlink video sharing scenario," *IEEE Trans. Wireless Commun.*, vol. 15, no. 2, pp. 1575–1587, Feb. 2016.

[8] J. Du, E. Gelenbe, C. Jiang, H. Zhang, and Y. Ren, "Contract design for traffic offloading and resource allocation in heterogeneous ultra-dense networks," *IEEE J. Sel. Areas Commun.*, vol. 35, no. 11, pp. 2457–2467, Nov. 2017.

[9] J. Wang, C. Jiang, Z. Bie, T. Q. S. Quek, and Y. Ren, "Mobile data transactions in device-to-device communication networks: Pricing and auction," *IEEE Wireless Commun. Lett.*, vol. 5, no. 3, pp. 300–303, Jun. 2016.

[10] C.-H. Yu, K. Doppler, C. B. Ribeiro, and O. Tirkkonen, "Resource sharing optimization for device-to-device communication underlaying cellular networks," *IEEE Trans. Wireless Commun.*, vol. 10, no. 8, pp. 2752–2763, Aug. 2011.

[11] G. Yu, L. Xu, D. Feng, R. Yin, G. Y. Li, and Y. Jiang, "Joint mode selection and resource allocation for device-to-device communications," *IEEE Trans. Commun.*, vol. 62, no. 11, pp. 3814–3824, Nov. 2014.

[12] D. Wu, J. Wang, R. Q. Hu, Y. Cai, and L. Zhou, "Energy-efficient resource sharing for mobile device-to-device multimedia communications," *IEEE Trans. Veh. Technol.*, vol. 63, no. 5, pp. 2093–2103, Jun. 2014.

[13] D. D. Penda, L. Fu, and M. Johansson, "Mode selection for energy efficient D2D communications in dynamic TDD systems," in *Proc. ICC*, London, U.K., Jun. 2015, pp. 5404–5409.

[14] T. D. Hoang, L. B. Le, and T. Le-Ngoc, "Energy-efficient resource allocation for D2D communications in cellular networks," *IEEE Trans. Veh. Technol.*, vol. 65, no. 9, pp. 6972–6986, Sep. 2016.

[15] Z. Zhou. M. Dong, K. Ota, R. Shi, Z. Liu, and T. Sato, "Game-theoretic approach to energy-efficient resource allocation in device-to-device underlay communications," *IET Commun.*, vol. 9, no. 3, pp. 375–385, 2015.

[16] Z. Zhou, M. Dong, K. Ota, G. Wang, and L. T. Yang, "Energy-efficient resource allocation for D2D communications underlaying cloud-RAN-based LTE-A networks," *IEEE Internet Things J.*, vol. 3, no. 3, pp. 428–438, Jun. 2016.

[17] Z. Zhou, M. Dong, K. Ota, J. Wu, and T. Sato, "Energy efficiency and spectral efficiency tradeoff in device-to-device (D2D) communications," *IEEE Wireless Commun. Lett.*, vol. 3, no. 5, pp. 485–488, Oct. 2014.

[18] B. Bhardwaj and S. Agnihotri, "Energy- and spectral-efficiency tradeoff for D2D-multicasts in underlay cellular networks," *IEEE Wireless Commun. Lett.*, vol. 7, no. 4, pp. 546–549, Aug. 2014.

[19] Z. Zhang, Y. Li, C.-X. Wang, Y. Ruan, Y. Fu, and H. Zhang, "Energy-spectral efficiency trade-off in underlaying mobile D2D communications: An economic efficiency perspective," *IEEE Trans. Wireless Commun.*, vol. 17, no. 7, pp. 4288–4301, Jul. 2018.

[20] S. Andreev, A. Pyattaev, K. Johnsson, O. Galinina, and Y. Koucheryavy, "Cellular traffic offloading onto network-assisted device-to-device connections," *IEEE Commun. Mag.*, vol. 52, no. 4, pp. 20–31, Apr. 2014.

[21] Z. Wang and V. W. S. Wong, "A novel D2D data offloading scheme for LTE networks," in *Proc. ICC*, London, U.K., Jun. 2015, pp. 3107–3112.

[22] Y. Li, Z. Wang, D. Jin, and S. Chen, "Optimal mobile content downloading in device-to-device communication underlaying cellular networks," *IEEE Trans. Wireless Commun.*, vol. 13, no. 7, pp. 3596–3608, Jul. 2014.

[23] T. Wang, Y. Sun, L. Song, and Z. Han, "Social data offloading in D2D-enhanced cellular networks by network formation games," *IEEE Trans. Wireless Commun.*, vol. 14, no. 12, pp. 7004–7015, Dec. 2015.

[24] L. Al-Kanj, H. V. Poor, and Z. Dawy, "Optimal cellular offloading via device-to-device communication networks with fairness constraints," *IEEE Trans. Wireless Commun.*, vol. 13, no. 8, pp. 4628–4643, Aug. 2014.

[25] Y. Li, D. Jin, P. Hui, and Z. Han, "Optimal base station scheduling for device-to-device communication underlaying cellular networks," *IEEE J. Sel. Areas Commun.*, vol. 34, no. 1, pp. 27–40, Jan. 2016.

[26] N. Lee, X. Lin, J. G. Andrews, and R. W. Heath, Jr., "Power control for D2D underlaid cellular networks: Modeling, algorithms and analysis," *IEEE J. Sel. Areas Commun.*, vol. 33, no. 1, pp. 1–13, Jan. 2015.

[27] Q. Ye, M. Al-Shalash, C. Caramanis, and J. G. Andrews, "Resource optimization in device-to-device cellular systems using time-frequency hopping," *IEEE Trans. Wireless Commun.*, vol. 13, no. 10, pp. 5467–5480, Oct. 2014.

[28] X. Lin, J. G. Andrews, and A. Ghosh, "Spectrum sharing for device-to-device communication in cellular networks," *IEEE Trans. Wireless Commun.*, vol. 13, no. 12, pp. 6727–6740, Dec. 2014.

[29] H. ElSawy, E. Hossain, and M. S. Alouini, "Analytical modeling of mode selection and power control for underlay D2D communication in cellular networks," *IEEE Trans. Commun.*, vol. 62, no. 11, pp. 4147–4161, Nov. 2014.

[30] S. Stefanatos, A. G. Gotsis, and A. Alexiou, "Operational region of D2D communications for enhancing cellular network performance," *IEEE Trans. Wireless Commun.*, vol. 14, no. 11, pp. 5984–5997, Nov. 2015.

[31] G. Zhao, S. Chen, L. Zhao, and L. Hanzo, "Energy-spectral-efficiency analysis and optimization of heterogeneous cellular networks: A large-scale user-behavior perspective," *IEEE Trans. Veh. Technol.*, vol. 67, no. 5, pp. 4098–4112, May 2018.
[32] Y. Li, S. Su, and S. Chen, "Social-aware resource allocation for device-to-device communications underlaying cellular networks," *IEEE Wireless Commun. Lett.*, vol. 4, no. 3, pp. 293–296, Jun. 2015.
[33] C. Gao, Y. Li, Y. Zhao, and S. Chen, "A two-level game theory approach for joint relay selection and resource allocation in network coding assisted D2D communications," *IEEE Trans. Mobile Comput.*, vol. 16, no. 10, pp. 2697–2711, Oct. 2017.
[34] C. Gao, H. Zhang, X. Chen, Y. Li, D. Jin, and S. Chen, "Impact of selfishness in device-to-device communication underlying cellular networks," *IEEE Trans. Veh. Technol.*, vol. 66, no. 10, pp. 9338–9349, Oct. 2017.
[35] J. G. Andrews, F. Baccelli, and R. K. Ganti, "A tractable approach to coverage and rate in cellular networks," *IEEE Trans. Commun.*, vol. 59, no. 11, pp. 3122–3134, Nov. 2011.
[36] S.-R. Cho and W. Choi, "Energy-efficient repulsive cell activation for heterogeneous cellular networks," *IEEE J. Sel. Areas Commun.*, vol. 31, no. 5, pp. 870–882, May 2013.
[37] E. Björnson, L. Sanguinetti, J. Hoydis, and M. Debbah, "Optimal design of energy-efficient multi-user MIMO systems: Is massive MIMO the answer?" *IEEE Trans. Wireless Commun.*, vol. 14, no. 6, pp. 3059–3075, Jun. 2015.
[38] R. L. Streit, *Poisson Point Processes: Imaging, Tracking and Sensing*. New York, NY, USA: Springer, 2010.
[39] S. Srinivasa, "Modeling interference in uniformly random wireless networks: Theory and applications," M.S. thesis, Dept. Elect. Eng., Univ. Notre Dame, Notre Dame, IN, USA, 2007.
[40] J. Ferenc, and Z. Néda, "On the size distribution of Poisson-Voronoi cells," *Phys. A, Stat. Mech. Appl.*, vol. 385, no. 2, pp. 518–526, 2007.

Guogang Zhao received the Ph.D. degree from the Department of Telecommunication Engineering, Xidian University. From 2015 to 2017, he was a Visiting Ph.D. Student under the guidance of Prof. L. Hanzo and Prof. S. Chen with the School of Electronics and Computer Science, University of Southampton, U.K. Since 2018, he has been with Zhengzhou University. His research interests focus on next-gwireless communication, network planning, and ultra-dense cellular networks.

Sheng Chen (M'90–SM'97–F'08) received the B.Eng. degree in control engineering from the East China Petroleum Institute, Dongying, China, in 1982, the Ph.D. degree in control engineering from City University, London, in 1986, and the D.Sc. degree (the higher doctoral degree) from the University of Southampton, Southampton, U.K., in 2005. From 1986 to 1999, he held research and academic appointments at the Universities of Sheffield, Edinburgh, and Portsmouth, all in U.K. Since 1999, he has been with the School of Electronics and Computer Science, University of Southampton, where he holds the post of Professor in intelligent systems and signal processing. He is also a Distinguished Adjunct Professor at King Abdulaziz University, Jeddah, Saudi Arabia, and an original ISI highly cited researcher in engineering (March 2004). He has published over 650 research papers. He has over 13,000 Web of Science citations and over 27,000 Google Scholar citations. His research interests include adaptive signal processing, wireless communications, modeling and identification of nonlinear systems, neural networks and machine learning, intelligent control system design, and evolutionary computation methods and optimisation. He is a fellow of the United Kingdom Royal Academy of Engineering and the IET.

Lin Qi received the B.Sc. degree in radio engineering from the Nanjing University of Posts and Telecommunications, Nanjing, China, the M.A.Sc. degree in computer science from Zhengzhou University, Zhengzhou, China, and the Ph.D. degree in information and communication engineering from the Beijing Institute of Technology, Beijing, China. He is currently a Professor with the School of Information Engineering, Zhengzhou University. His current research interests include image and video analysis and processing, pattern recognition, and signal detection and estimation.

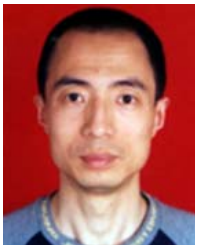

Liqiang Zhao received the B.Eng. degree in electrical engineering from Shanghai Jiao Tong University, China, in 1992, and the M.Sc. degree in communications and information systems and the Ph.D. degree in information and communications engineering from Xidian University, China, in 2000 and 2003, respectively. From 1992 to 2005, he was a Senior Research Engineer with the 20th Research Institute, Chinese Electronics Technology Group Corporation (CETC), China. From 2005 to 2007, he was an Associate Professor with the State Key Laboratory of Integrated Service Networks (ISN), Xidian University. Since 2008, he returned Xidian University, where he holds the Professor in information and communication engineering. His research focused on mobile communication systems and spread spectrum communications, WiMAX, WLAN, and wireless sensor network. He was appointed as a Marie Curie Research Fellow at the Centre for Wireless Network Design (CWiND), University of Bedfordshire, in 2007, to conduct research in the GAWIND project funded under EU FP6 HRM programme. His activities focused on the area of automatic wireless broadband access network planning and optimization. His current research focuses on 5G, aerospace communications, and nano-networks. Since 2005, he has been awarded over 20 projects funded by a number of sources, government and direct industrial funding. His participation in various projects has yielded a number of concrete results including enormous high-level publications. Due to his excellent works in education and research. He was awarded by the Program for New Century Excellent Talents in University, Ministry of Education, China, in 2008.

Lajos Hanzo (F'04) received the D.Sc. degree in electronics in 1976 and the Ph.D. degree in 1983. During his 40-year career in telecommunications, he has held various research and academic posts in Hungary, Germany, and U.K. Since 1986, he has been with the School of Electronics and Computer Science, University of Southampton, U.K., where he holds the Chair of telecommunications. He is currently directing an academic research team, working on a range of research projects in the field of wireless multimedia communications sponsored by industry, the Engineering and Physical Sciences Research Council (EPSRC) U.K., the European Research Council's Advanced Fellow Grant, and the Royal Society's Wolfson Research Merit Award. He is an enthusiastic supporter of industrial and academic liaison and he offers a range of industrial courses. He has successfully supervised 120 Ph.D. students, coauthored 18 John Wiley/IEEE Press books on mobile radio communications totaling in excess of 10,000 pages, published 1840 research contributions at the IEEE Xplore. He is fellow of the IET, EURASIP, and a FREng. He received an Honorary Doctorate from the Technical University of Budapest in 2009 and The University of Edinburgh in 2015. In 2016, he was admitted to the Hungarian Academy of Science. He is also a Governor of the IEEE VTS. He served as the TPC Chair and the General Chair for the IEEE conferences, presented keynote lectures, and has been awarded a number of distinctions. From 2008 to 2012, he was the Editor-in-Chief of the IEEE Press and a Chaired Professor also at Tsinghua University, Beijing. For further information on research in progress and associated publication please refer to http://wwwmobile.ecs.soton.ac.uk.